
ADVERSARIAL NETWORK TRAFFIC: TOWARD EVALUATING THE ROBUSTNESS OF DEEP LEARNING BASED NETWORK TRAFFIC CLASSIFICATION

A PREPRINT

Amir Mahdi Sadeghzadeh

Department of Computer Engineering
Sharif University of Technology
amsadeghzadeh@ce.sharif.edu

Rasool Jalili

Department of Computer Engineering
Sharif University of Technology
jalili@sharif.edu

Saeed Shiravi

Department of Computer Engineering
Sharif University of Technology
shiravi@ce.sharif.edu

ABSTRACT

Network traffic classification is used in various applications such as network traffic management, policy enforcement, and intrusion detection systems. Although most applications encrypt their network traffic and some of them dynamically change their port numbers; Machine Learning (ML) and especially Deep Learning (DL)-based classifiers have shown impressive performance in network traffic classification. In this paper, we evaluate the robustness of DL-based network traffic classifiers against Adversarial Network Traffic (ANT). ANT causes DL-based network traffic classifiers to predict incorrectly using Universal Adversarial Perturbation (UAP) generating methods. We partition the input space of the DL-based network traffic classification into three categories: Packet Classification (PC), Flow Content Classification (FCC), and Flow Time Series Classification (FTSC). To generate ANT, we propose three new attacks injecting UAPs to the network traffic. AdvPad attack injects a UAP into the content of packets to evaluate the robustness of packet classifiers. AdvPay attack injects a UAP into the payload of a dummy packet to evaluate the robustness of flow content classifiers. AdvBurst attack injects a specific number of dummy packets with crafted statistical features based on a UAP into a selected burst of a flow to evaluate the robustness of flow time series classifiers. The results indicate injecting a little UAP to the network traffic, highly decreases the performance of DL-based network traffic classifiers in all categories.

Keywords Network Traffic Classification, Adversarial Network Traffic, Adversarial Example.

1 Introduction

In recent years, Internet traffic has grown due to the emergence of new applications and services in market. Hence, management of network traffic is more challenging than ever. The necessity of network traffic classification is obvious in many cases, such as quality of service provision, resource usage management, billing in ISPs, anomaly identification, malware detection, and Policy Enforcement. So far, three main approaches of network traffic classification have been introduced, including port-based, payload-based, and ML-based classification[1, 2].

In the early stage of the Internet, most applications used well-known port numbers, and most traffic classification tasks were solved by extracting port numbers from TCP/UDP headers and assigning them to the predefined list introduced by Internet Assigned Numbers Authority (IANA) [3]. This method is still being used in various devices such as firewalls due to high speed and simple implementation[4]. Although the port-based approach has prevailed in many devices, it

has low success rate because of dynamic port allocation, port forwarding, and tunneling. Also, an adversary can use random port numbers or well-known port numbers to evade port-based classifiers[5].

Payload-based approach, also known as Deep Packet Inspection (DPI), tries to extract specific patterns from the content of packets. DPI methods search for specific signatures in the network traffic and match predefined patterns to the extracted content of packets. Although this approach has high computational overhead for regular expression matching, it has higher accuracy in comparison to the port-based approach and looks more promising, encountering the problem of port-based approaches. However, the success rate of this approach is decreased in encrypted network traffic. An adversary can encrypt his/her network traffic or obfuscate the pattern in the content of packets to evade the payload-based classifiers[2, 5].

The third approach utilizes ML-based algorithms for network traffic classification. The byte sequence and statistical features of packets or flows are the most common features that are used by ML-based network traffic classifiers. ML-based classifiers have a training phase and a prediction phase. In the training phase, they learn a mapping from the input space to the output space, while in the prediction phase, they predict the class of a new data, which has not been seen in the training phase. Although ML-based approaches have been put forward with claims of fixing the problems of previous approaches, the robustness of ML-based classifiers has not been evaluated. In this paper, we will investigate the robustness of such classifiers in a comprehensive way.

In recent years, Deep Neural Networks (DNNs), also called Deep Learning (DL), have shown great success in solving complex problems such as image classification [6], speech recognition [7], and playing Go [8]. These advances have motivated the researchers to use DNNs in other domains, and recently, researchers have demonstrated the DNNs have promising results in the network traffic classification [9, 10, 11, 12, 13, 14]. Besides, an essential stage in traditional ML-based classifiers has been feature engineering. In this stage, an specialist tries to extract the most prominent features of data, such as variance, mean of inter-arrival times between packets [10, 15], or entropy of the byte sequence of packets [16]. Using DNNs as the classifier, not only the feature engineering step is set aside but also it is done along with classification. In this paper, we focus on DL-based network traffic classifiers, which are state of the art in ML-based network traffic classification.

Based on the previous studies, we divide the input space of DL-based network traffic classification into three categories: Packet Classification (PC), Flow Content Classification (FCC), and Flow Time Series Classification (FTSC). In PC, the byte sequence of a packet is given to a classifier, and each packet is labeled. In FCC, the byte sequence of the first n packets of a flow is fed to a classifier, and the class of each flow is predicted. In FTSC, the sequence of the statistical features of the first m packets of a flow, such as packets size and inter-arrival times between packets, are passed to a classifier, and each flow is labeled. To assess the influence of the transport layer header in PC and FCC, and various statical features in FTSC, we consider two classifiers in each input space category. In PC, the first classifier is PC-HP, which takes the byte sequence of the transport layer header as well as the payload, and the second one, PC-P only takes the payload of each packet as the input. In FCC, the first classifier FCC-HP is fed by the byte sequence of the transport layer header as well as the payload of the first n packets, and the second one, FCC-P is only fed by the byte sequence of the payload of the first n packets of a flow. In FTSC, the first classifier FTSC-PS uses the time series of the size of first m packets in a flow, and the second one, FTSC-IAT uses the time series of inter-arrival times between first m packets in a flow to classify network flows. In this paper, we use One-Dimensional Convolutional Neural Networks (1D-CNN) to classify ISCXVPN2016 dataset [15] in which multiple application, including Skype, Facebook, and Hangouts generate network traffic with different characters. The target of network traffic classification in this study is traffic characterization in which the character of network traffic such as VoIP, streaming, email, and chat is determined.

After the success of DNNs in various classification tasks, their robustness has become the subject of much debate [17]. In 2014, Szegedy *et al.* [18] have demonstrated that DNNs are vulnerable to adversarial examples, which are maliciously crafted inputs that cause the classifier to make a mistake. The primary method for generating an adversarial example is adding a crafted adversarial perturbation to a natural data, which in most cases, the size of adversarial perturbation is limited [19, 20, 21, 22]. Papernot *et al.* [23] have indicated that adversarial examples are transferable among different ML algorithms and also among classifiers with different training sets. This vulnerability questioned the robustness of DL-based classifiers in the adversarial environment in which an adversary can interfere in the training and the prediction phase. In this paper, the robustness of DL-based network traffic classifiers against Adversarial Network Traffic (ANT) is evaluated using the idea of adversarial example. ANT is crafted network traffic in which the content or the statistical features of network traffic is perturbed, and it is independent of the application that generates network traffic and does not disrupt the functionality of applications.

There are some constraints to generate ANT: (*i*) the content of packets must be preserved; otherwise, the functionality of network traffic might be disrupted, (*ii*) in some character such as VoIP, email, and chat, the content and statistical features of a flow are generated over time and are dependent to the user, and there is no access to the entire flow at the

beginning of it, *(iii)* A flow is generated by two entity, and neither of them knows the content and the statistical features of entire flow to make adversarial perturbation based on it, and *(iv)* making adversarial perturbation for each flow or packet have high computation overhead. According to these constraints, we use Universal Adversarial Perturbation (UAP) generating methods to generate ANT. Moosavi-Dezfooli *et al.* [24] demonstrate that there is a perturbation that, if it is added to a set of data, it will cause DNNs to make incorrect predictions on most of them, and this perturbation is not unique. In ANT, the UAP is generated on a pre-collected set of network traffic, and whenever a new flow or a new packet is being sent, the pre-made UAP is injected into it. This approach does not need to have access to the entire data to make perturbation based on it, and the UAP is crafted beforehand on the pre-collected set of network traffic.

In this paper, three new attacks for generating ANT are proposed, including Adversarial Pad (AdvPad) attack, Adversarial Payload (AdvPay) attack, and Adversarial Burst (AdvBurst) attack. The AdvPad attack injects a UAP into the end or the start of packets payload to evaluate the robustness of packet classifiers PC-HP and PC-P. The AdvPay attack injects a UAP into the payload of a dummy packet at the first n packets of a flow to evaluate the robustness of flow content classifiers FCC-HP and FCC-P. The AdvBurst attack injects a specific number of dummy packets with crafted statistical features based on a UAP into the end of a selected burst of a flow to evaluate the robustness of flow time series classifier FTSC-PS and FTSC-IAT. The experiments show that all six classifiers are vulnerable to ANT, and by injecting a little adversarial perturbation to the network traffic, the performance of DL-based network traffic classifiers highly decreases. The results of this paper demonstrate that the researchers should investigate the methods for improving the robustness of DL-based network traffic classifiers.

The contributions of this paper are as follow:

- Network traffic is formally defined, including packets, unidirectional flows, bidirectional flows, and three input space categories of DL-based network traffic classifiers.
- The influence of the input space category on the performance and robustness of the DL-based network traffic classifiers is investigated, and also the effect of transport layer header on the performance and robustness of PC and FCC is examined.
- Adversarial Network Traffic (ANT) is proposed to evaluate the robustness of DL-based network traffic classifiers and use Universal Adversarial Perturbation (UAP) to generate ANT due to constraints in the network traffic classification task.
- Three new attacks are proposed to generate ANT. The AdvPad attack evaluates the robustness of packet classifiers PC-P and PC-HP. The AdvPay attack evaluates the robustness of flow content classifiers FCC-P and FCC-HP. The AdvBurst attack evaluates the robustness of flow time series classifiers FTSC-PS and FTSC-IAT.

The rest of the paper is organized as follows. In Sec. 2, the network traffic, and the input space categories of DL-based network traffic classification are formally defined. Also, the DNNs and basic methods for generating adversarial examples are introduced. Sec. 3 reviews the related works on DL-based network traffic classification. In Sec. 4, ANT will be presented, and the AdvPad, the AdvPay, and the AdvBurst attacks are proposed. Sec. 5 evaluates the robustness of three input space categories classifiers against the three proposed attacks. Finally, in Sec. 7, the conclusions of this work will be discussed.

2 Background

Network traffic and DL-based classifiers are the fundamental constituents of the DL-based network traffic classification task. Accordingly, in the following subsections, we first formally specify network traffic and general concepts of network traffic classification, including input space, output space, and machine learning classifiers will be introduced. Then, some central concepts of the deep neural network will be expressed, and at last, an introduction to adversarial examples and some essential methods for generating them are presented.

2.1 Formal Specification of Network Traffic

Network traffic consists of bidirectional flows and packets, which are the common objects for network traffic classification. Each packet consists of multiple headers and a payload in which application data exists. Headers have particular information about source and destination of the packet, the route, the session state, as well as the state of source and destination machine. In this paper, we indicate the headers of a packet by 5-tuple information, which stems from the contents of the IP layer and Transport Layer (TL) headers.

Definition 1. A packet P_i is a sequence of an IP layer header, a TL header, and a payload.

$$\begin{aligned} P_i &= \langle H_{P_i}^{IP}, H_{P_i}^{TL}, Pay_{P_i} \rangle, \\ H_{P_i}^{IP} &= (IP_{P_i}^{src}, IP_{P_i}^{dst}), \\ H_{P_i}^{TL} &= (Port_{P_i}^{src}, Port_{P_i}^{dst}, Proto_{P_i}) \end{aligned} \quad (1)$$

where $IP_{P_i}^{src}$ and $IP_{P_i}^{dst}$ indicate source and destination IP addresses of the packet, respectively. $Port_{P_i}^{src}$ and $Port_{P_i}^{dst}$ are source and destination ports of the transport layer, respectively, and $Proto_{P_i}$ is the transport layer protocol of the packet. Unidirectional flow is a set of packets that share the same source and destination information and transport layer protocol.

Definition 2. A unidirectional flow UF_i is a set of an IP layer header, a TL header, and a sequence of packets.

$$\begin{aligned} UF_i &= \{H_{UF_i}^{IP}, H_{UF_i}^{TL}, P_{UF_i}\}, \\ H_{UF_i}^{IP} &= (IP_{UF_i}^{src}, IP_{UF_i}^{dst}), \\ H_{UF_i}^{TL} &= (Port_{UF_i}^{src}, Port_{UF_i}^{dst}, Proto_{UF_i}), \\ P_{UF_i} &= \langle P_1^i, P_2^i, \dots, P_m^i \rangle, \\ s.t. H_{P_j^i}^{IP} &= H_{UF_i}^{IP} \text{ and } H_{P_j^i}^{TL} = H_{UF_i}^{TL}, \quad 1 \leq j \leq m. \end{aligned} \quad (2)$$

where m is the number of packets in unidirectional flow UF_i and $IP_{UF_i}^{src}$ and $IP_{UF_i}^{dst}$ are source and destination IP addresses of unidirectional flow UF_i , respectively. $Port_{UF_i}^{src}$ and $Port_{UF_i}^{dst}$ are source and destination ports of the transport layer, respectively, and $Proto_{UF_i}$ is the transport layer protocol of unidirectional flow UF_i . Bidirectional flow is the union of two unidirectional flows, where IP addresses and ports have switched.

Definition 3. A bidirectional flow BF_i is the union of two opposite unidirectional flow UF_j and UF_k .

$$\begin{aligned} BF_i &= UF_j \cup UF_k, \\ s.t. IP_{UF_j}^{src} &= IP_{UF_k}^{dst} \text{ and } IP_{UF_j}^{dst} = IP_{UF_k}^{src} \text{ and} \\ Port_{UF_j}^{src} &= Port_{UF_k}^{dst} \text{ and } Port_{UF_j}^{dst} = Port_{UF_k}^{src} \text{ and} \\ Proto_{UF_j} &= Proto_{UF_k} \end{aligned} \quad (3)$$

For simplicity, we use flow instead of bidirectional flow in the rest of the paper.

2.2 ML-Based Network Traffic Classification

ML classifier is a function $Func$ which maps an input space \mathcal{X} to an output space $\mathcal{Y} = \{y_1, \dots, y_k\}$ where y_i is i^{th} class, and k is the number of classes. Given an input $x_i \in \mathcal{X}$, the classifier assigns it to one of the k classes. In the training phase of a classifier, we need to have a training set in which the true class of each sample has been given $\{(x_i, y_i)\}_{i=1}^n$, where n is the number of samples in the train set and y_i is the true class (label) of the sample x_i . The classifier uses this set to estimate the true concept \mathcal{C} of data by function $Func$, and quality of classification depends on the closeness of $Func$ and \mathcal{C} . A good classifier generalizes to unseen samples and classifies them correctly. Therefore, we should have a test set similar to the training set that the classifier has not been trained on yet, and this set is used to evaluate the performance of classifier. We have divided the input space of network traffic classification into three categories: (i) packet classification (PC), (ii) flow content classification (FCC), and (iii) flow time series classification (FTSC).

According to the previous studies, the output space of network traffic classification involves many targets, including protocol, application, video, website, and character. Nevertheless, three principal targets in network traffic classification are protocol detection, application identification, and traffic characterization. In protocol detection, the protocol of network traffic, such as HTTP, FTP, and SMTP, tends to be determined. Whereas, in application identification, traffic is classified based on the application that generates traffic, such as Facebook, Skype, or Netflix. In this paper, we focus on traffic characterization, which specifies the character of network traffic, such as VoIP, streaming, file transferring, and email. To the best of our knowledge, at least one of the input space categories has good accuracy on each target, and regarding our purpose in this study, it is not important which target is chosen. Nevertheless, we think traffic characterization is fundamental in many scenarios, such as network traffic accounting, quality of service providing, and policy enforcement systems. Since the information in the header of the IP layer is dependent on the machines that generate network traffic, we do not consider IP header for network traffic classification. Moreover, if classifiers utilize

the information in the header of the IP layer to classify network traffic, then by changing the condition of network, the performance of classifiers drops down. In what follows, each input space category will be explained.

Packet Classification (PC). In packet classification, the byte sequence of a packet is given to the classifier, and it labels each packet separately. Based on the literature, we consider two versions of packet classification. In the first version (PC-HP), DL-classifier is fed with TL header and payload of a packet while in the later version (PC-P), only payload is given. For packet P_i , we have:

$$\begin{aligned} \text{PC-HP Input for } P_i: & \langle H_{p_i}^{TL}, \text{Pay}_{p_i} \rangle . \\ \text{PC-P Input for } P_i: & \langle \text{Pay}_{p_i} \rangle . \end{aligned} \quad (4)$$

Often, the input size of classifier is fixed and all data inputs of DL-based classifier must have the same size. Hence, we add zero pad to the end of packets until their length reaches $MaxPktSize$.

Flow Content Classification (FCC). In this category, the byte sequence of the first n packets of a flow is given to a classifier, and each flow is labeled. Previous studies have shown that using only the first packets of a flow is enough for classifying flows with high accuracy. Furthermore, classifying flows using just the first few packets is useful for online policy enforcement systems. Likewise PC, FCC has two versions. In the first version (FCC-HP), TL headers and payloads, and in the second one (FCC-P), only payloads of the first n packets are given to a classifier. To improve the performance of classifiers, we multiply the sign of the packet direction to the content of that packet. The direction sign is considered positive (+1) for packets from source (e.g., client) to destination (e.g., server) and negative (-1) for packets from destination to source. For flow F_i , we have:

$$\begin{aligned} \text{FCC-HP Input for } F_i: & \langle H_{p_0}^{TL} \times D_{p_0}^i, \text{Pay}_{p_0}^i \times D_{p_0}^i, \dots, H_{p_{n-1}}^{TL} \times D_{p_{n-1}}^i, \text{Pay}_{p_{n-1}}^i \times D_{p_{n-1}}^i \rangle, \\ \text{FCC-P Input for } F_i: & \langle \text{Pay}_{p_0}^i \times D_{p_0}^i, \dots, \text{Pay}_{p_{n-1}}^i \times D_{p_{n-1}}^i \rangle, \end{aligned} \quad (5)$$

where $D_{p_j}^i \in \{+1, -1\}$ is j^{th} packet direction of flow F_i . Since classifier inputs must be the same size, we add zero pad to the end of each packet until the length of the packet reaches $MaxPktSize$. If a flow has less than n packets, we add zero pad to the end of the byte sequence until length of the byte sequence become $n \times MaxPktSize$ bytes.

Flow Time Series Classification (FTSC). There have been various attempts to classify traffic using statistical features of flow such as packet size and inter-arrival time. In FTSC, the statistical features of the first m packets of a flow are given to a classifier. If a flow has less than m packets, relevant features of nonexistent packets are assumed as zero. Two versions of FTSC have been considered in the previous studies. In the first version (FTSC-IAT), inter-arrival times between packets of a flow, and in the second version (FTSC-PS), packets sizes of a flow are given to the classifier in time-series format. Similar to FCC, we multiply the sign of packets direction to the statistical features of packets to improve the performance of the classifiers. For flow F_i , we have:

$$\begin{aligned} \text{FTSC-IAT Input for } F_i: & \langle IAT_{(p_0^i, p_1^i)} \times D_{p_1^i}, IAT_{(p_1^i, p_2^i)} \times D_{p_2^i}, \dots, IAT_{(p_{m-2}^i, p_{m-1}^i)} \times D_{p_{m-1}^i} \rangle \\ \text{FTSC-PS Input for } F_i: & \langle PS_{p_0^i} \times D_{p_0^i}, PS_{p_1^i} \times D_{p_1^i}, \dots, PS_{p_{m-1}^i} \times D_{p_{m-1}^i} \rangle \end{aligned} \quad (6)$$

Where $IAT_{(p_j^i, p_k^i)}$ is inter-arrival time between j^{th} and k^{th} packets, $D_{p_j^i} \in \{+1, -1\}$ is j^{th} packet direction, and $PS_{p_j^i}$ is size of j^{th} packet in flow F_i .

2.3 Deep Neural Networks

Deep neural networks (DNNs) have achieved great success in network traffic classification, and have outperformed classic machine learning algorithms such as decision tree, support vector machine, and k-nearest neighbors. Likewise other machine learning classifiers, DNN are a function $y_i = f_{DNN}(x_i)$ which takes an input $x_i \in \mathcal{X}$ and returns an output $y_i \in \mathcal{Y}$. DNNs include multiple layers which through early layers, the features of input are extracted, and the last layers do reasoning on the output of previous layers. DNNs act on raw data and do not need feature engineering. Therefore, there is no need to have feature selection or an expert who extracts the most salient features for network traffic classification.

Convolutional Neural Network (CNN), Recurrent Neural Network (RNN), and Stacked Denoising Autoencoders (SDAE) are the three main DNNs which have been used in network traffic classification. Previous investigations [14, 11, 12, 25] have demonstrated that a One-Dimensional Convolutional Neural Network (1D-CNN) have delivered the best performance in network traffic classification. In this paper, we use 1D-CNN to classify network traffic.

CNNs have shown excellent performance in tasks in which local information of data is decisive for the classification task (e.g., image classification and face recognition). The favorable performance of CNNs on network traffic shows

local information in network traffic plays a primary role in network traffic classification. In what follows, a formal and brief review of the neural network has been explained shortly.

Each neural network includes an input layer, multiple hidden layers, and an output layer. Each layer consists of multiple neurons that are connected to neurons in the adjacent layers. The size (number of neurons) of the input layer is equal to the dimension of input data, and the size of the output layer is equal to the number of classes k . In a fully connected neural network, except for the input layer, the output of a given layer is calculated through applying a nonlinear function on an obtained value from multiplying the output of previous layer by the weights matrix of that layer. For a deep neural network f_{DNN} with l layers and an input x , we have:

$$\begin{aligned} f_{DNN}^i(x^i) &= \sigma(\theta^i \times x^i + b^i) \\ f_{DNN}(x) &= f_{DNN}^{l-1}(f_{DNN}^{l-2}(\dots, f_{DNN}^1(x))) \end{aligned} \quad (7)$$

where, $f_{DNN}^i(x)$ is the output of i^{th} layer, x^i is the input of the i^{th} layer, σ is a non-linear function, θ^i is the weights matrix of i^{th} layer, and b_i is the bias vector of i^{th} layer. Notice, the output of the first layer (input layer) is the input x . The softmax function is often used as a non-linear function of the last layer to compute the output of the neural network. Hence, the output of the neural network is a non-negative k -size vector which sum of elements is one. A DNN assigns the label $\hat{y} = \operatorname{argmax}_{0 \leq i < k} f_{DNN}(x)_i$ to the input x , where $f_{DNN}(x)_i$ is the i^{th} element of DNN output.

The output of the penultimate layer f_{DNN}^{l-1} is termed logits.

The deep convolutional neural network f_{DCNN} uses filters for weight sharing, and in each layer, filters convolve on the given input. Given a one-dimensional input of size N and a one-dimensional filter of size M , the n^{th} element of the i^{th} layer output $f_{DCNN}^{i,n}$ is:

$$f_{DCNN}^{i,n}(x) = \sum_{m=0}^{M-1} \sigma(\theta_m^i \times x_{n+m} + b_m^i), \quad s.t. 0 \leq n \leq N - M \quad (8)$$

where, θ_m^i is the m^{th} element of i^{th} layer's filter weights, x_{n+m} is the $(n+m)^{th}$ element of i^{th} layer input, and b_m^i is the m^{th} element of i^{th} layer filter bias. The weights union of all layers is called $\theta = \bigcup_{i=2}^l \theta_i$, and in the training phase, these weights are adjusted to minimize a loss function J . J measures the distance between predicted label \hat{y} by a classifier and the true label y of data. Often, the true label y is given to the loss function as a one-hot vector in which the element corresponds to the true class is set as one whereas others are considered as zero. Hence, training is a minimization problem on the weights of classifier. The output of the training phase is θ^* that minimizes the loss function J . We have:

$$\theta^* = \operatorname{argmin}_{\theta} J(\theta, x, y) \quad (9)$$

Since DNNs are non-convex function, finding θ^* is hard. Stochastic gradient descent (SGD) and its versions are used for the minimization of the loss function in DNNs. SGD changes the weights of DNNs towards the opposite direction of the loss function gradient to decrease loss function in each step. SGD is an iterative algorithm, and in each iteration, DNN's weights θ are updated by the computed gradients of the loss function with respect to θ . We have:

$$\theta^{t+1} = \theta^t - \eta \nabla_{\theta^t} J(\theta^t, x, y) \quad (10)$$

where, θ^t is weights of DNN at t^{th} iteration, η is learning rate which tunes the size of change in weights, and $\nabla_{\theta^t} J(\theta, x, y)$ is the gradient of loss function J with respect to θ^t .

Previous studies have used batch normalization, dropout, and polling layer to improve the performance of DNNs in network traffic classification. By normalizing the output of hidden layers, batch normalization enhances the stability of DNNs. Polling layers decrease the size of their input and prevent DNNs from over-fitting by reducing the size of DNNs. Max-polling layer is one of the most common polling layers, which only passes the max element in its filter. Dropout is a regularization technique, and in each training iteration, randomly deletes some neurons and prevents DNNs from overfitting to the training set (For more information, see [26]).

2.4 Adversarial Example

Although DNNs have achieved great success in solving complex problems, it has serious vulnerability called adversarial example. An adversarial example is a crafted input which causes the target classifier to make a mistake. Suppose that a classifier f_{unc}^* assigns true label to each data. For an adversarial example x' , we have:

$$\begin{aligned} f_{unc}^*(x') &= y, \\ f_{unc}(x') &= y', \quad s.t. y' \neq y \end{aligned} \quad (11)$$

while y is the true class of x' , the target classifier $func$ assigns a label $y' \neq y$ to it. Szedgy *et al.* [18] have shown for the first time that adding an imperceptible perturbation to an image changes output of a DNN classifier. The main method for creating an adversarial example is adding an adversarial perturbation ξ to a real data x . In this method, it is supposed that after adding perturbation to data x , the true class of $x' = x + \xi$ and x must be the same. Given that a large perturbation can change the true class of data, the amount of perturbation has to be limited in many contexts (e.g., image and voice classification). In image classification, the actual class of an image is dependent on the intensity of pixels, and if an adversary adds a significant perturbation to them, the true class of image alters. Hence, the size of the perturbation should be controlled with some distant functions.

The most common distant function is used in the literature is $L_p = \|x' - x\|_p$ where x is a real image, x' is adversarial example, and the P -norm is defined as:

$$\|d\|_p = \left(\sum_{i=0}^{D-1} |d_i|^p \right)^{1/p} \quad (12)$$

where D is the dimension of data d . Generation of adversarial example can be formulated as a minimization problem:

$$\begin{aligned} & \text{minimize } \|x' - x\|_p \\ & \text{s.t. } func^*(x') = y \text{ and } func(x') = y' \text{ and } y' \neq y \\ & \text{and } x' \in Domain(x) \end{aligned} \quad (13)$$

Goodfellow *et al.* [20] propose Fast Gradient Sign Method (FGSM) attack to solve the minimization problem. Authors use the gradient of DNN loss function to compute the adversarial perturbation, and L_∞ to limit the size of perturbation. The L_∞ distance metric confines the shifting range of perturbation to ϵ towards each of its dimensions. In FGSM, adversarial perturbation is calculated as follow:

$$\xi = \epsilon \cdot sign(\nabla_x J(\theta, x, y)) \quad (14)$$

where $\nabla_x J(\theta, x, y)$ is the gradient of DNN loss function with respect to input x . In the training phase of DNN, we compute the gradient of the loss function with respect to weights of a classifier, and by moving weights towards the opposite direction of the gradients, the value of loss function for the true class y is decreased. However, in FGSM, the gradient of the loss function is calculated with respect to the input, and by moving the input towards the direction of the gradient, the loss of true class y rises. Thereby, by increasing the loss value for the true class, likely DNN assigns the label of the wrong class to an adversarial example.

Kurakin *et al.* [27] propose an iterative gradient sign (IGS) attack in which instead of taking one step with size ϵ , they take multiple steps with size α , which is smaller than ϵ . Authors applied *clip* function to limit the maximum change of each dimension to ϵ . In the first step, $x'_0 = x$, and in each iteration:

$$\begin{aligned} \xi_t &= \alpha \cdot sign(\nabla_x J(\theta, x'_t, y)) \\ x'_{t+1} &= clip_\epsilon(x'_t + \xi_t) \end{aligned} \quad (15)$$

Authors demonstrate that adversarial examples crafted by IGS outperform FGSM in terms of the size of perturbation, aiming to fool the classifier.

Moosavi-Dezfooli *et al.* [24] introduce a Universal Adversarial Perturbation (UAP) attack, which is different from previous attacks. In previous attacks, a perturbation is made for each data. However, the UAP attack adds a single perturbation ξ^u to a set of data and hops that they would be misclassified with a high probability of $1 - \delta$. This attack has two constraints:

$$\begin{aligned} \|\xi^u\|_p &< \epsilon \\ P_{x \in \mathcal{X}}(func(x + \xi^u) \neq func(x)) &\geq 1 - \delta \end{aligned} \quad (16)$$

To generate UAP, the authors used an iterative algorithm. In iteration $t > 0$, a data x is sampled from \mathcal{X} and ξ_{t-1}^u is added to the data x . Then, the perturbation r is calculated using the following equation ($\xi_0^u = 0$).

$$\begin{aligned} r_t &= \underset{r}{\operatorname{argmin}} \|r\|_2 \\ \text{s.t. } func(x + \xi_{t-1}^u + r) &\neq func(x) \end{aligned} \quad (17)$$

To calculate ξ_t^u , r_t is added to ξ_{t-1}^u in each iteration, and authors have used a projection function $\mathcal{P}_{p,\epsilon}(v)$, which maps the input v to a L_p ball of radius ϵ and is centered at zero to ensure that the constraint $\|\xi^u\|_p < \epsilon$ is satisfied. Therefore:

$$\xi_t^u = \mathcal{P}_{p,\epsilon}(\xi_{t-1}^u + r_t) \quad (18)$$

Authors have demonstrated that there is no need to have much data to generate universal adversarial perturbation, and this perturbation is not unique.

3 Related Works

The DL-based network traffic classification has been widely studied in the literature, and a brief review of previous studies are introduced in this section. Based on the category of input space, the studies is explained in separate sections. Table 1 provides an overview of previous studies.

3.1 Packet Classification

Lotfollahi *et al.* present the Deep Packet framework that embeds stacked autoencoder and convolutional neural networks to classify network traffic [14]. Their framework reduces manual efforts for feature engineering, and they claim that the Deep packet outperform all of the similar works on ISCXVPN2016 dataset. The Deep Packet uses the byte sequence of the transport layer header and the payload of packets to classify packets. Regarding their claim, this work is the first try to perform both application identification and traffic characterization by a DL-based classifier. The results show that the 1D-CNN classifier has better overall performance rather than SDAE in both application identification and traffic characterization, and the overall accuracy of the 1D-CNN in application identification is 98%, and the precision in traffic characterization is 93%.

P. Wang *et al.* introduce a DL-based encrypted traffic classifier called Datanet for better management of distributed smart home networks and aiding the software-defined-network (SDN) controller in real-time network traffic monitoring and classification [28]. In the first step, packets are preprocessed, and after removing the header of the Data-link layer, the byte sequence of packets is fed to the Datanet. Same as [14], Datanet uses ISCXVPN2016 dataset and reaches the F-measure $\geq 96\%$ for both the SDAE and CNN in distinguishing 15 applications.

3.2 Flow Content Classification

The first study to apply deep learning in network traffic classification is introduced by Z. Wang *et al.* [29]. They recognize remarkable feature engineering ability of deep learning and try to detect protocols in a TCP flow dataset by means of SDAE. Their dataset consists of 300k pre-processed records in which exist 1000 bytes of TCP payload. They achieve more than 90% recall in protocol detection for all protocols.

W. Wang *et al.* propose an end-to-end encryption traffic classifier for traffic characterization [25]. They use ISCXVPN2016 dataset and extract only 728 bytes of each flow as the input. The authors have shown that the 1D-CNN has better performance rather than 2D-CNN in network traffic classification. Also, they investigate the influence of headers and the type of flows in network traffic classification. The result of their study shows that including headers in the input improves the performance of the network traffic classifier, and the classifier has better performance on bidirectional flows rather than unidirectional flows. They achieve the best result in the classification of the ISCXVPN2016 dataset compared to previous works that use the classical ML algorithms. In another work, they identify malware traffic using the same approach, by transforming raw traffic data to image and using 2D-CNN as a spatial feature learner [30].

After several studies in the domain of mobile application identification [31, 32], Aceto *et al.* addressed mobile application identification through the Deep Learning approach for the first time[11]. They investigate type of input data that is fed to the DL-classifier and consider three types of input data: (i) first N bytes of payload in a flow, (ii) first N bytes of all headers and payloads in a flow, and (iii) source and destination ports, number of bytes in the transport-layer header, TCP window size, inter-arrival time, and direction of packets in a flow. Although results demonstrate the classifier, which is trained on the second type of input data, has the best performance, the authors claim that the results of this classifier are biased to the information in headers and hence not meaningful. The performance of the classifier is trained on the first type of input data is better than the classifier is trained on the third type of input data, and they achieve 83% overall accuracy for identifying 45 applications in both Android and IOS operating systems. Also, they demonstrate that the overall performance of 1D-CNN and 2D-CNN are close in mobile application identification and suggest that traffic should be extracted by naturally considering data as one-dimensional.

3.3 Flow Time Series Classification

In [15], authors utilize a set of time-related features such as duration of flow, byte per second, and inter-arrival times of packets for network traffic classification. They use C4.5 and K-nearest neighbors as classification techniques and achieve about 80% accuracy in the characterization of network traffics. Moreover, they generate and distribute a labeled dataset of encrypted network traffic is called ISCXVPN2016, which has become a criterion in network traffic classification.

Table 1: Overview of previous studies.

Input Space Category	Paper	Input data	Classifier	Classification Target	Year
PC	P. Wang <i>et al.</i> [28]	$H^{IP}, H^{TL}, payload$	SDAE,MLP,CNN	Application identification	2018
	M. Lotfollahi <i>et al.</i> [14]	$H^{TL}, payload$	SDAE,CNN	Application identification, Traffic characterization	2017
FCC	Z. Wang <i>et al.</i> [29]	$H^{TL}, payload$	SDAE	Protocol detection	2015
	W. Wang <i>et al.</i> [25]	$H^{IP}, H^{TL}, payload$	CNN	Traffic characterization	2017
	W. Wang <i>et al.</i> [30]	$H^{IP}, H^{TL}, payload$	SDAE	Malware classification	2017
FCC-FTSC	G. Aceto <i>et al.</i> [11]	$H^{IP}, H^{TL}, payload, IAT, PS, Dir$	SDAE,CNN	Application identification	2019
FTSC	J. Caicedo-Muñoz <i>et al.</i> [10]	Time-related features	Bagging, Boosting	Traffic characterization	2018
	G. Draper-Gi <i>et al.</i> [15]	Time-related Features	KNN,C4.5	Traffic characterizaion	2016
	M. López Martín <i>et al.</i> [9]	PS, Dir, H^{TL}	LSTM,CNN	Protocol detection	2017
	K. Abe and S. Goto [33]	Dir, IAT	SDAE	Website classification	2016
	V. Rimmer <i>et al.</i> [13]	Dir	SDAE,CNN,LSTM	Website classification	2017
	P. Sirinam <i>et al.</i> [12]	Dir	CNN	Website classification	2018
	S. Rezaie and X. Liu [34]	IAT, PS, Dir	CNN	Application identification	2018

In [10] authors improve the performance of [15], and achieve about 83% accuracy on ISCXVPN2016 dataset using bagging and boosting classifiers. Since these two studies use the time-related features of the entire flow to classify network traffic, their approaches are not useful in online policy enforcement systems.

Rezaei and Liu propose a semi-supervised approach based on a 1D-CNN to classify five Google applications [34]. They train a 1D-CNN to predict the statistical features of the entire flow from a few sampled packets on a large unlabeled dataset. Then, they transfer the 1D-CNN to a new classifier and add some fully connected layers to the top of it. Afterward, the new classifier re-train on a few labeled samples for application identification task. They show the possibility of using sampled packets features instead of first n packets in network traffic classification, which is more feasible for high bandwidth operational networks.

Lopez-Martin *et al.* [9] introduce a new hybrid classifier based on CNN and RNN to detect services used by different devices with various user-profiles in IoT network traffic. In this work, each flow comprises 20 packets, and each packet contains six features, including source port, destination port, the number of bytes in the packet payload, TCP window size, inter-arrival time, and direction of packets. Regarding the results, whenever a RNN is combined with a CNN, success rate slightly improves, and the performance of the classifier decreases by including inter-arrival times in the input.

The process of identifying network traffic of visited websites through privacy-enhancing technologies like Tor, which is also known as Website Fingerprinting (WF), has a background as long as encrypted traffic classification. In this domain, besides that traffic is encrypted in multiple layers, the statistical feature of traffic obscured. Abe and Goto investigate the effectiveness of DL-based classifiers in WF for the first time [33]. In their experiment, network traffic of 100 websites that passed through Tor is monitored, and the statistical feature of each flow is extracted. They reveal that SDAE is useful in the detection of network traffic of 100 websites only using direction and inter-arrival times of cells (Tor packets) with an 86% success rate.

Rimmer *et al.* indicate that DL is an effective tool in automating the process of features engineering, and it can eliminate the need for feature design and selection. Their SDAE achieves a 95.3% success rate only using the direction of Tor cells [13]. In another work, Sirinam *et al.* design a deeper CNN classifier to outperform earlier studies, which increase the success rate to 98% [12]. These studies indicate that applying deep learning reduces the reliance on human insight for feature engineering, as well as notable improvement in the performance of WF classifiers.

4 Adversarial Network Traffic

Adversarial Network Traffic (ANT) evaluates the robustness of DL-based network traffic classifiers, using the concept of the adversarial example attack. In the adversarial example attack, an adversary adds a little perturbation into the

input data and causes the classifier to make a false prediction. In the same approach to deceive DL-based network traffic classifiers, ANT injects a perturbation to the network traffic. Most of the adversarial example attacks have been proposed in the context of image processing, and we can not directly use them in the context of network traffic classification. There are some constraints to apply adversarial example attacks in the context of network traffic classification.

1. The contents of packets must be preserved. If the content of a packet is modified, the functionality of the application that uses the packet is disrupted. Hence, we are not allowed to perturb the content of packets. The perturbation can only be injected into some specific parts of the input, such as the end of packets, or the content of a dummy packet.
2. In conventional machine learning tasks, like image classification, adversarial perturbation is made based on the entire data. However, in the traffic classification task, two entities make entire data, and neither of them has access to the entire data.
3. In some characters like chat, email, and VoIP, the application that generates network traffic is not aware of the content of network traffic at the beginning of a flow, and the content of network traffic is dependent on the user. Hence, there is no access to the entire flow at the beginning of it.
4. Making a perturbation for each packet or flow has high computational overhead.

Based on these constraints, ANT uses Universal Adversarial Perturbation (UAP) to cause the classifier to predict wrongly. In this approach, there is no need to have access to the entire new data to make adversarial perturbation, and there is no need to compute one perturbation for each input. Also, UAP is independent of the content of target data and is made on a pre-collected set of data. To make the UAP, first, a set of flows or packets of the character from which we want to make the UAP is collected, and after crafting the UAP, it injects into new incoming network traffic of that character. For example, at the first step, VoIP flows are collected, then a UAP for VoIP class is made using a pre-collected VoIP network traffic. Afterward, when a new VoIP flow is being sent, the UAP is injected into this flow to fool the DL-based network traffic classifier.

Based on the category of input space, the method of generating ANT and applying the UAP is different. In PC, a UAP is injected into the start or the end of the payload of the packet. This attack is called the adversarial pad attack (AdvPad). In FCC, a dummy packet is added to the early packets of a flow, and a UAP is injected into the content of this dummy packet. This attack is called the adversarial payload attack (AdvPay). In FTSC, a sequence of dummy packets having crafted statistical features is appended to the end of a selected burst of a flow. This attack is called the adversarial burst attack (AdvBurst). We explain these attacks in the following sections.

In this paper, we assume the adversary has white-box access to the DL-based classifiers. In the white-box setting, the adversary knows the input space category, the architecture, the weights of the deep learning classifier, and the outputs of the classifier. Nevertheless, Papernot *et al.* [23] have shown that adversarial examples are transferable between the different classifiers with different training data set. In the black-box setting, an adversary can use the proposed attacks and run them on the substitute classifier, which is close to the target classifier, and he/she uses the generated perturbation to evade the target classifier.

4.1 Adversarial Pad Attack

The adversarial pad (AdvPad) attack is designed to reduce the success rate of two previously introduced packet classifiers, PC-HP, and PC-P. The AdvPad attack injects a universal adversarial perturbation in the specific location of packets payload. We only consider the start and the end of the payload of the packet for injecting adversarial pad and call them Start_AdvPad and End_AdvPad Attacks, respectively. If UAP injects at the start of the payload, the structure of an adversarially padded packet P_i is as follow:

$$\begin{aligned} \text{PC-HP Input for } P_i: & \langle H_{P_i}^{TL}, AdvPad, Pay_{P_i} \rangle, \\ \text{PC-P Input for } P_i: & \langle AdvPad, Pay_{P_i} \rangle. \end{aligned} \tag{19}$$

If UAP injects at the end of the payload, the structure of an adversarially padded packet P_i is as follow:

$$\begin{aligned} \text{PC-HP Input for } P_i: & \langle H_{P_i}^{TL}, Pay_{P_i}, AdvPad \rangle, \\ \text{PC-P Input for } P_i: & \langle Pay_{P_i}, AdvPad \rangle. \end{aligned} \tag{20}$$

Algorithm 1 shows the process of making UAP for the AdvPad attack. This algorithm has T iterations, which in each iteration, a batch of packets are sampled from packets set P . All packets in P has the same label l . If the attack is run on PC-HP, the packets in P have payload and header, and if the attack is run on PC-P, the packets in P only have a

Algorithm 1 Universal Adversarial Pad

Input Packet set P of class l , packet classifier $func$ with weights θ , overhead percentage OH , perturbation rate ϵ , location of UAP Loc_{AdvPad} , number of iterations T , batch size $batch_size$.

Output Adversarial pad vector ξ

- 1: $\xi \leftarrow Rand(Domain(P), Size = MaxPktSize)$
- 2: **for** $t \leftarrow 0, T$ **do**
- 3: $P^{batch} \leftarrow sample\ batch_size\ packets\ from\ P$
- 4: **for** $i \leftarrow 0, batch_size$ **do**
- 5: $pad_size \leftarrow sizeof(p_i^{batch}) \times OH/100$
- 6: $\xi' \leftarrow \xi[0 : pad_size]$
- 7: **if** $Loc_{AdvPad} == Start$ and $func == PC - HP$ **then**
- 8: $packets_byte_sequence_i^{batch} \leftarrow \langle H_{p_i^{batch}}^{TL}, \xi', Pay_{p_i^{batch}} \rangle$
- 9: **else if** $Loc_{AdvPad} == Start$ and $func == PC - P$ **then**
- 10: $packets_byte_sequence_i^{batch} \leftarrow \langle \xi', Pay_{p_i^{batch}} \rangle$
- 11: **else if** $Loc_{AdvPad} == End$ and $func == PC - HP$ **then**
- 12: $packets_byte_sequence_i^{batch} \leftarrow \langle H_{p_i^{batch}}^{TL}, Pay_{p_i^{batch}}, \xi' \rangle$
- 13: **else if** $Loc_{AdvPad} == End$ and $func == PC - P$ **then**
- 14: $packets_byte_sequence_i^{batch} \leftarrow \langle Pay_{p_i^{batch}}, \xi' \rangle$
- 15: **end if**
- 16: **end for**
- 17: $\Delta\xi \leftarrow \epsilon \times \nabla_{\xi} J(\theta, packets_byte_sequence^{batch}, l)$
- 18: $\xi \leftarrow Clip_{Domain(P)}(\xi + \Delta\xi)$
- 19: **end for**
- 20: **return** ξ

payload. For i^{th} packet in the batch of packets p^{batch} , the UAP ξ is injected at the start or the end of the payload, the UAP location is specified by the parameter Loc_{AdvPad} . A bandwidth overhead parameter OH is considered to control the bandwidth overhead of the AdvPad attack. OH determines the percentage of bandwidth overhead that we want to add to each packet. Based on this parameter, we add the first pad_size bytes of ξ to the p_i^{batch} . In each iteration, the perturbation ξ is updated based on the following equations:

$$\begin{aligned} \Delta\xi &= \epsilon \times \nabla_{\xi} J(\theta, packets_byte_sequence^{batch}, l), \\ \xi &= Clip_{Domain(P)}(\xi + \Delta\xi), \end{aligned} \quad (21)$$

where $\nabla_{\xi} J(\theta, packets_byte_sequence^{batch}, l)$ is the loss function gradient with respect to ξ , and ϵ controls the magnitude of changes in ξ during each iteration. The function $Clip_{Domain(P)}(x)$ maps the input x to the packets domain $Domain(P)$ by clipping features that are not in it. In this attack, ξ is updated in the direction that increases the loss of the true class. Note that Algorithm 1 only generates adversarial pad ξ for one class l , and for creating an adversarial pad for each class, this algorithm must run on the packet set of each class, separately.

4.2 Adversarial Payload Attack

The adversarial payload (AdvPay) attack aims to deceive two flow content classifiers, FCC-HP and FCC-P, through adding the UAP to the payload of a dummy packet. As mentioned earlier, in FCC, flow classification is done using the first n packets of a flow. In AdvPay attack, a dummy packet is injected in a specified location $k \in [0, n - 1]$ among the first n packets of a flow, and UAP is injected into it. The direction of the dummy packet can be arbitrary; nonetheless, we choose the direction of the last packet before the dummy Packet $D_{p_{k-1}^i}$ as the direction of the dummy packet. The input of FCC-HP and FCC-P for flow F_i are changed as follow:

$$\begin{aligned} \text{FCC-HP Input for } F_i: & \langle H_{P_0^i}^{TL} \times D_{p_0^i}, Pay_{P_0^i} \times D_{p_0^i}, \dots, \\ & H_{P_k^i}^{TL} \times D_{p_{k-1}^i}, AdvPay_{P_k^i} \times D_{p_{k-1}^i}, \dots, H_{P_{n-2}^i}^{TL} \times D_{p_{n-2}^i}, Pay_{P_{n-2}^i} \times D_{p_{n-2}^i} \rangle \quad (22) \\ \text{FCC-P Input for } F_i: & \langle Pay_{P_0^i} \times D_{p_0^i}, \dots, AdvPay_{P_k^i} \times D_{p_{k-1}^i}, \dots, Pay_{P_{n-2}^i} \times D_{p_{n-2}^i} \rangle \end{aligned}$$

Algorithm 2 generates UAP that is used as an adversarial payload in this attack. In FCC-HP, the flow set F consists of the transport layer header and the payload of packets, and in FCC-P, it only consists of the payload of packets. The

Algorithm 2 Universal Adversarial Payload

Input Flow set F of class l , flow content classifier $func$ with weights θ , dummy packet index vector IND_{Advpay}
AdvPay size $AdvPaysize$, perturbation rate ϵ , number of iterations T , batch size $batch_size$.
Output Adversarial payload vector ξ

- 1: $\xi \leftarrow 0$ with size $AdvPaysize$
- 2: **for** $t \leftarrow 0, T$ **do**
- 3: $F^{batch} \leftarrow \text{sample } batch_size \text{ flows from } F$
- 4: $IND^{batch} \leftarrow \text{get dummy packet index of flows in } F^{batch} \text{ from } IND_{Advpay}$
- 5: **for** $i \leftarrow 0, batch_size$ **do**
- 6: $flows_byte_seq_i^{batch} \leftarrow \langle \rangle$
- 7: **for** $j \leftarrow 0, n-1$ **do**
- 8: **if** $j < k$ **then**
- 9: $flows_byte_seq_i^{batch} \leftarrow \langle flows_byte_seq_i^{batch}, P_j^{F^{batch}} \times D_j^{F^{batch}} \rangle$
- 10: **else if** $j == k$ **then**
- 11: $flows_byte_seq_i^{batch} \leftarrow \langle flows_byte_seq_i^{batch}, \text{dummy packet which carries UAP } \xi \times D_{j-1}^{F^{batch}} \rangle$
- 12: **else if** $j > k$ **then**
- 13: $flows_byte_seq_i^{batch} \leftarrow \langle flows_byte_seq_i^{batch}, P_{j-1}^{F^{batch}} \times D_{j-1}^{F^{batch}} \rangle$
- 14: **end if**
- 15: **end for**
- 16: **end for**
- 17: $\Delta\xi = \epsilon \times \nabla_{\xi} J(\theta, flows_byte_seq^{batch}, l)$
- 18: $\xi = Clip_{Domain(F)}(\xi + \Delta\xi)$
- 19: **end for**
- 20: **return** ξ

AdvPay packet index vector IND_{AdvPay} is considered to determine the location of the dummy packet in the flow. For example, it can be the first or the second packet from source to destination or any other location in the first n packets of a flow. Algorithm 2 has T iterations, and in each iteration, $batch_size$ flows from the flow set F is sampled F^{batch} to update AdvPay ξ . For each batch, first, a dummy packet that carries UAP ξ with size $AdvPaysize$ bytes is injected into the byte sequence of flows in the batch $flows_byte_seq^{batch}$, and afterward, the AdvPay ξ is updated as follow:

$$\begin{aligned} \Delta\xi &= \epsilon \times \nabla_{\xi} J(\theta, flows_byte_seq^{batch}, l) \\ \xi &= Clip_{Domain(F)}(\xi + \Delta\xi) \end{aligned} \quad (23)$$

where $\nabla_{\xi} J(\theta, flow_byte_seq^{batch}, l)$ is the loss function gradient with respect to ξ and ϵ tunes the change of ξ in each iteration. The function $Clip_{Domain(F)}$ maps ξ to the domain of byte sequence of flows by clipping the value of the AdvPay ξ and controls the direction sign of the dummy packet.

4.3 Adversarial Burst Attack

The flow time series contains the statistical features of the packets in the order which they are received. A burst in the flow is a sequence of consecutive packets in one direction. The inputs FTSC-IAT and FTSC-PS for flow F_i can be expressed using the concept of bursts as follow:

$$\begin{aligned} \text{FTSC-IAT and FTSC-PS Inputs for } F_i: & \langle (Brs_0^i, D_0^i), (Brs_1^i, D_1^i), \dots, (Brs_n^i, D_n^i) \rangle \\ \text{s.t. } D_j^i & \in \{-1, +1\}, D_j^i = -1 \times D_{j+1}^i, j \in [0, n-1], \end{aligned} \quad (24)$$

where n is the number of bursts in flow F_i and (Brs_j^i, D_j^i) is defined as follows for FTSC-IAT and FTSC-PS:

$$\begin{aligned} (Brs_j^i, D_j^i) \text{ for FTSC-PS: } & \langle PS_{p_0^j} \times D_{p_0^j}, PS_{p_1^j} \times D_{p_1^j}, \dots, PS_{p_m^j} \times D_{p_m^j} \rangle \\ (Brs_j^i, D_j^i) \text{ for FTSC-IAT: } & \langle IAT_{(p_{m'}^{(j-1)}, p_0^j)} \times D_{p_0^j}, IAT_{(p_0^j, p_1^j)} \times D_{p_1^j}, \dots, IAT_{(p_{m-1}^j, p_m^j)} \times D_{p_m^j} \rangle \\ \text{s.t. } D_{p_k^j} & \in \{-1, +1\}, D_{p_k^j} = D_j^i, k \in [0, m], \end{aligned} \quad (25)$$

where m is the number of packets in the Brs_j^i , $p_{m'}^{(j-1)}$ is the last packet of $Brs_{(j-1)}^i$ and if j is 0 then the $IAT_{(p_{m'}^{(j-1)}, p_0^j)}$ will be 0. In the Adversarial Burst (AdvBurst) attack, multiple dummy packets with crafted statistical features are

Algorithm 3 Universal Adversarial Burst

Input Flow set F of class l , flow content classifier $func$ with weights θ , selected burst index vector IND_{SBurst} , number of dummy packet $Num_of_dummy_pkts$, perturbation rate ϵ , number of iterations T , batch size $batch_size$.

Output Adversarial burst vector ξ

- 1: $\xi \leftarrow Rand(Domain(F), Size = Num_of_dummy_pkts)$
- 2: **for** $t \leftarrow 0, T$ **do**
- 3: $F^{batch} \leftarrow sample\ batch_size\ flows\ from\ F$
- 4: $IND^{batch} \leftarrow get\ selected\ burst\ index\ of\ flows\ in\ F^{batch}\ from\ IND_{SBurst}$
- 5: **for** $i \leftarrow 0, batch_size$ **do**
- 6: $flows_time_series_i^{batch} \leftarrow flow_to_burst_sequence(F_i^{batch})$
- 7: $Brs_s^i = flows_time_series_i^{batch}[IND_i^{batch}]$
- 8: $Brs_{adv}^i = \langle Brs_s^i, \xi \rangle$
- 9: $flows_time_series_i^{batch}[IND_i^{batch}] = Brs_{adv}^i$
- 10: **end for**
- 11: $\Delta\xi = \epsilon \times \nabla_{\xi} J(\theta, flows_time_series^{batch}, l)$
- 12: $\xi = Clip_{Domain(F)}(\xi + \Delta\xi)$
- 13: **end for**
- 14: **return** ξ

added to the end of a selected burst. First, a burst Brs_s^i from the flow F_i is selected, and then, d dummy packets are appended to the end of it. The direction of dummy packets and the selected burst Brs_s^i are the same. The sequence of dummy packets $\langle p_1^{dummy}, p_2^{dummy}, \dots, p_d^{dummy} \rangle$ and the selected burst Brs_s^i build a new burst Brs_{adv}^i . The statistical features of dummy packets are based on UAP. After applying the AdvBurst attack, the structure of flow F_i is as follows:

$$F_i: \langle (Brs_0^i, D_0^i), (Brs_1^i, D_1^i), \dots, (Brs_{s-1}^i, D_{s-1}^i), (Brs_{adv}^i, D_s^i), \dots, (Brs_n^i, D_n^i) \rangle \quad (26)$$

where (Brs_{adv}^i, D_s^i) for FTSC-IAT and FTSC-PS is defined as follow:

$$\begin{aligned} (Brs_{adv}^i, D_s^i) \text{ for FTSC-PS: } & \langle PS_{p_0^s} \times D_{p_0^s}, \dots, PS_{p_m^s} \times D_{p_m^s}, PS_{p_0^{dummy}} \times D_s^i, \dots, PS_{p_d^{dummy}} \times D_s^i \rangle \\ (Brs_{adv}^i, D_s^i) \text{ for FTSC-IAT: } & \langle IAT_{(p_{m'}^{s-1}, p_0^s)} \times D_{p_0^s}, \dots, IAT_{(p_{m-1}^s, p_m^s)} \times D_{p_m^s}, IAT_{(p_m^s, p_0^{dummy})} \times D_s^i, \dots, \\ & IAT_{(p_{d-1}^{dummy}, p_d^{dummy})} \times D_s^i, \rangle \end{aligned} \quad (27)$$

where Brs_s^i is the selected burst, and m is the number of packets in the selected burst. Algorithm 3 generates UAP that the AdvBurst attack uses as the statistical features of dummy packets. To specify the place of adversarial burst in each flow, this algorithm gets the adversarial burst indices vector IND_{SBurst} , which determines the indices of the selected burst in each flow. Algorithm 3 runs in T iterations. In each iteration, $batch_size$ number of flows are sampled F^{batch} , and the selected burst indices of these flows are determined by IND^{batch} . Afterward, the batch of flows is transformed into burst sequences $flows_time_series^{batch}$, and the selected burst of each flow Brs_s^i is replaced by the adversarial burst Brs_{adv}^i . The number of dummy packets that are added to the end of the selected burst is specified by $Num_of_dummy_pkts$ parameter. The parameter ξ is updated according to the following equations:

$$\begin{aligned} \Delta\xi &= \epsilon \times \nabla_{\xi} J(\theta, flows_time_series^{batch}, l) \\ \xi &= Clip_{Domain(F)}(\xi + \Delta\xi) \end{aligned} \quad (28)$$

where $\nabla_{\xi} J(\theta, flows_time_series^{batch}, l)$ is the gradient of loss function with respect to ξ , and ϵ controls the rate of change in ξ during each iteration. The function $Clip_{Domain(F)}$ makes sure that the perturbation ξ is in the domain of statistical features of flow, and it also makes sure that the sign of ξ is the same as the dummy packets direction.

5 Evaluation

Three attacks have been proposed based on the category of input space in order to evaluate the robustness of the DL-based network traffic classifiers. In this section, the robustness of six different classifiers is examined against ANT. We scrutinize the robustness of packets classifiers against AdvPad attack, flow content classifiers against AdvPay attack,

and flow time series classifier against AdvBurst attack. Moreover, the robustness of classifiers that get the transport layer header as the input, PC-HP, and FCC-HP, are evaluated against the port attack. In the port attack, the port numbers of flows are randomly assigned from a specific range of port numbers. In the following, first, the network traffic dataset is introduced, and then, the metrics for evaluating the performance of a classifier is presented. Finally, the robustness of the classifiers based on the three categories of input space is investigated in separate sections.

5.1 Dataset

DL-based network traffic classifiers need to have a labeled set of network traffic in the training phase. Labeling is a tedious process because of the separation complexity of various classes of network traffic (even for a human), background network traffic, and the volume of network traffic. Some of the past studies have used deep packet inspection tools for labeling network traffic [35]. However, in these studies, the performance of the classifier depends on the performance of the deep packet inspection tool which is used to label the network traffic. The DL-based classifiers came to overcome the weaknesses of previous classifiers like deep packet inspection classifiers, and using them to supervise DL-based classifiers is a paradox. The privacy issue is another challenge that does not let the researchers share their network traffic datasets. Most of the public network traffic datasets only have statistical features of flows, not the content of them. Based on our knowledge, there are a few studies that have a reliable labeling process, and some of them have not enough data to train a deep neural network. To evaluate the robustness of DL-based network traffic classifiers, we need to access a dataset that shares content and statistical features of network traffic and has an adequate number of data to train a deep neural network.

Draper *et al.* [15] have presented ISCXVPN2016 dataset that consists of six characters, and some of the flows in the dataset are sent through a VPN. They use different applications such as Skype, Facebook, Hangouts, Youtube, and Bittorrent, to generate traffic with different characters, including chat, email, file transfer, streaming, torrent, and VoIP. This dataset has been labeled based on application and character, which have generated given network traffic. This dataset is highly imbalanced, and some of the classes like chat and email have less data than others. The dataset requires a preprocessing phase to clean some background traffic such as DNS and NETBIOS network traffics. Since there are three categories of input spaces, data padding, and normalization of each category is different. Hence, we discuss dataset properties of each category in a separate section.

5.2 Performance Metrics

Typical performance metrics for evaluating a classifier are precision, recall, and F-score. Based on the true label of data, the output of a classifier is divided into four groups, true-positive (TP), true-negative (TN), false-positive (FP), and false-negative (FN). The recall shows what fraction of given class data, classified correctly. The precision for a given label denotes what fraction of data is correctly classified (label confidence). F-score is a combination of precision and recall and indicates how fine are these both metrics. The equations are as follow:

$$Precision = \frac{TP}{TP + FP}, \quad Recall = \frac{TP}{TP + FN}, \quad F\text{-score} = \frac{2}{Precision^{-1} + Recall^{-1}}.$$

These three metrics are only used for data of one class. However, overall accuracy is used as a classifier performance metric on all classes data, and the overall accuracy of n-classes classifier defined as follow:

$$OverallAccuracy = \frac{TP_1 + TP_2 + \dots + TP_n}{Number\ of\ all\ classes\ data},$$

where TP_i is the number of true positive data of i^{th} class. Since proposed attacks cause the classifiers to misclassify data of a given class, the number of true-positive data of that class decreases, and consequently, the number of false-negative data of that class increases. As an example, if an attack makes a classifier misclassify chat data, then the number of true-positive data of this class decreases, and the number of false-negative data of this class increases. The proposed attacks do not change the number of false-positive data. Hence, we focus on recall and overall accuracy metrics in the evaluation section.

5.3 Packet Classification

In this section, we evaluate the robustness of packet classifiers against the port and the adversarial pad (AdvPad) attacks. To assess the effectiveness of the AdvPad attack, we propose a random pad attack (RandPad) as a baseline for evaluation of the AdvPad attack. In the RandPad attack, a random pad is injected into the payload of packets. The AdvPad attack must have a better performance than the RandPad attack. In the next section, we describe the dataset that is used to train packet classifiers, and also, we introduce the normalization and padding steps that are needed to prepare the dataset to train classifiers. Afterward, the packet classifiers are introduced, and finally, the robustness of packet classifiers against the AdvPad, the RandPad, and the port attacks is investigated.

Table 2: Packet classification dataset.

Character	Imbalanced Dataset		Undersampled Dataset		Oversampled Dataset	
	Dataset Quantity	Training Set Quantity	Dataset Quantity	Training Set Quantity	Dataset Quantity	Training Set Quantity
Chat	68,867	41,320	68,867	41,320	87,544	60,000
Email	30,930	18,558	30,930	18,558	72,372	60,000
Filetransfer	313,916	188,349	100,000	60,000	100,000	60,000
Streaming	124,487	74,692	100,000	60,000	100,000	60,000
Torrent	162,479	97,487	100,000	60,000	100,000	60,000
VoIP	596,476	357,885	100,000	60,000	100,000	60,000
Total	1,297,155	778,291	499,797	299,878	559,916	360,000

Table 3: Performance metrics of the packet classifiers, PC-HP, and PC-P.

Characture	PC-HP			PC-P		
	Precision(%)	Recall(%)	F-score(%)	Precision(%)	Recall(%)	F-score(%)
Chat	85.35	76.45	80.66	74.11	47.31	57.75
Email	65.77	75.35	70.23	59.97	69.84	64.53
FileTransfer	98.41	90.23	94.14	67.51	77.19	72.03
Streaming	79.96	91.50	85.34	48.08	41.88	44.77
Torrent	99.3	99.97	99.63	69.66	77.33	73.29
VoIP	87.24	84.47	85.83	76.33	85.15	80.50

5.3.1 Packet Classification Dataset

Packet classification dataset consists of the byte sequence of packets that have at least one byte of payload, and packets that have no payload are ignored. To prepare the packet classification dataset, we need to normalize the dataset. Since the decimal domain of each byte of the packet is in $[0,255]$ interval, we divide the decimal value of each byte by 255. Hence, each packet becomes a sequence of numbers between zero and one. Also, we need to add zero pad to the end of packets until their length reaches to $MaxPktSize$. In undersampling, a certain amount of data is sampled from a class and is put on the dataset. In oversampling, a certain amount of data from a class in the dataset is sampled and is replicated on the dataset until the amount of data for that class reaches a specific number. Based on the amount of data in each class, we choose 100,000 packets per each class, of which 60% are in the training set, 20% are in the validation set, and 20% are in the test set. Therefore each class must have 60,000 training samples, and if a class has more samples than this threshold, we sample 60,000 data from it, and if a class has less data than this threshold, we sample data from that class and add them to the training set until the number of training samples of that class reaches to this threshold. Table 2 shows the number of samples in each class.

5.3.2 Packet classifiers Setup

A 1D-CNN has been used to classify the byte sequences of packets. Given our computational resources, we trained almost fifty 1D-CNNs with different architectures and hyper-parameters, and finally, the classifier with higher accuracy on validation data has been selected. The architecture and hyper-parameters of the selected classifier are presented in Table 7 in Appendix A. As mentioned in section 2.2, we trained two classifiers, which the input of the first classifier (PC-HP) is byte sequence of the transport-layer header and the payload of a packet, and the input of the second model (PC-P) is only byte sequence of the payload of packets. The overall accuracies are 88.09% and 66.71% for PC-HP and PC-P, respectively. The precision, recall, and F-score of these classifiers are reported in Table 3. Because of information in the transport layer header of packets, PC-HP has higher performance than PC-P. PC-HP classifier performance is lower than the performance that has been reported in [14, 28]. We investigated this difference and found out that in their threat model, they split packets of one flow between train and test set. Since we do not have access to the labeled packets of the flow that classifier wants to classify its packets, this threat model is not practical in the real world. If our classifier trains on the dataset that packets of a flow are split between train and test set, its overall accuracy is 95.2%.

5.3.3 Packet Classifiers Robustness Evaluation

To evaluate the robustness of the packet classifiers, the port, the random pad (RandPad), and the adversarial pad (AdvPad) attacks are applied to them. The AdvPad attack has been conducted for 5000 iterations with $batch_size =$

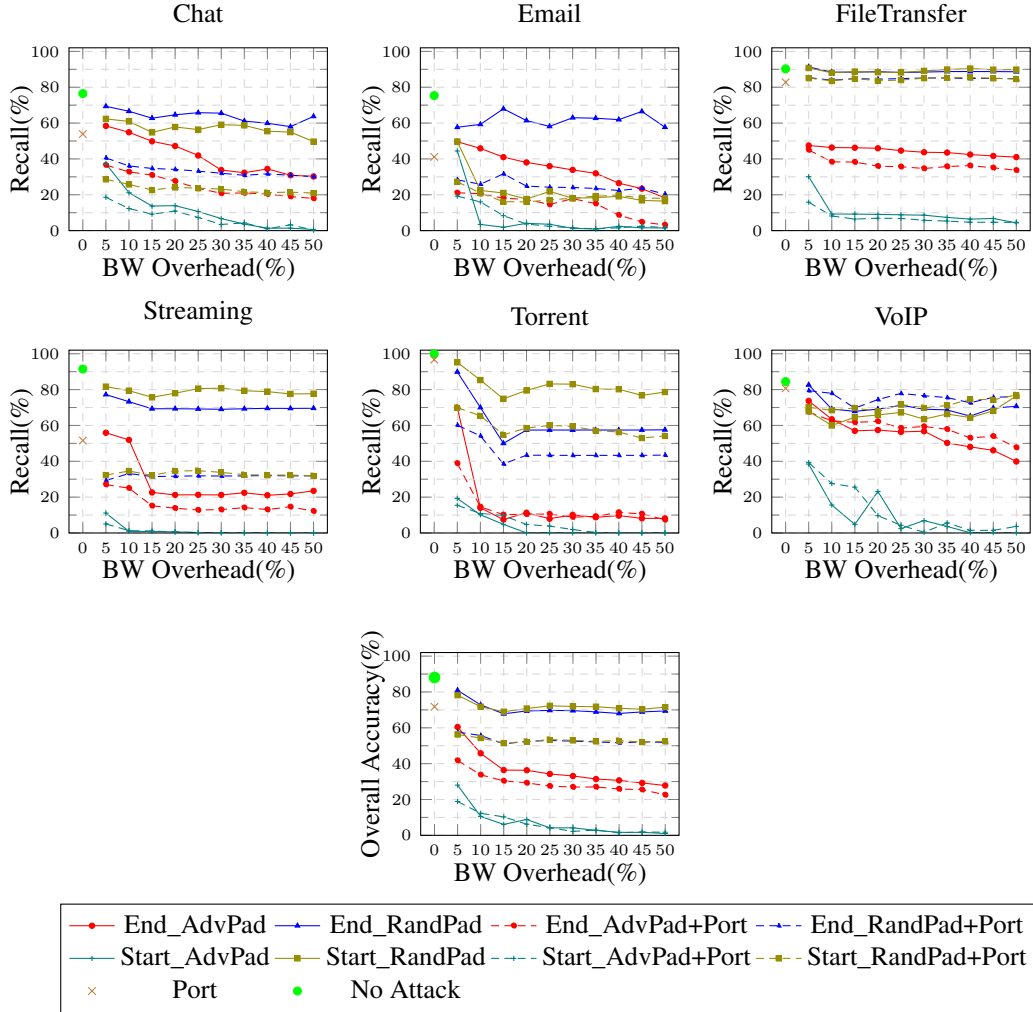


Figure 1: The recall of each class and the overall accuracy of PC-HP under different attacks over various sizes of BandWidth (BW) overhead. The legends show the kind of attacks that have been applied to PC-HP.

128 and $\epsilon=0.01$. For each class, Algorithm 1 generates a universal adversarial perturbation on the validation set with the desired percent of bandwidth overhead. Afterward, by injecting this perturbation as the adversarial payload in the test set, the robustness of packet classifiers has been evaluated. As an example, Algorithm 1 generates a universal adversarial perturbation on chat packets in the validation set with 5% Figure 1 shows the recall of each class and overall accuracy of PC-HP classifier under proposed attacks for the various magnitude of the BandWidth (BW) overhead. The precision and F-score of PC-HP under those attacks are presented in Figure 7 and Figure 8 in Appendix B.

The port attack randomly changes the transport layer port of flows, and it does not impose any BW overhead on the traffic. This attack decreases the overall accuracy of PC-HP from 88.09% to 71.73%. The recall of chat, email, and streaming classes decreases considerably under the port attack that shows PC-HP is highly sensitive to the transport-layer port numbers for classifying these classes. However, the port attack has little effect on the recall of other classes. We think the sensitivity of the classifier to the transport-layer port numbers depends on the intrinsic structure and the diversity of transport-layer port numbers in the data of a class.

The End_AdvPad attack injects the adversarial pad into the end of packets payload. This attack decreases the overall accuracy of PC-HP from 88.09% to 60.46% with just 5% BW overhead, and if it combines with the port attack (End_AdvPad+Port), the overall accuracy decreases to 41.76%. By increasing the BW overhead of the End_AdvPad and End_AdvPad+Port attacks, first, the decreasing rate of overall accuracy is high, and when reaching 20% BW overhead, this rate decreases. Finally, with 50% BW overhead, the overall accuracy of PC-HP decreases to 27.8% under the End_AdvPad attack, and to 22.6% under the End_AdvPad+Port attack. Also, by increasing the BW overhead, the

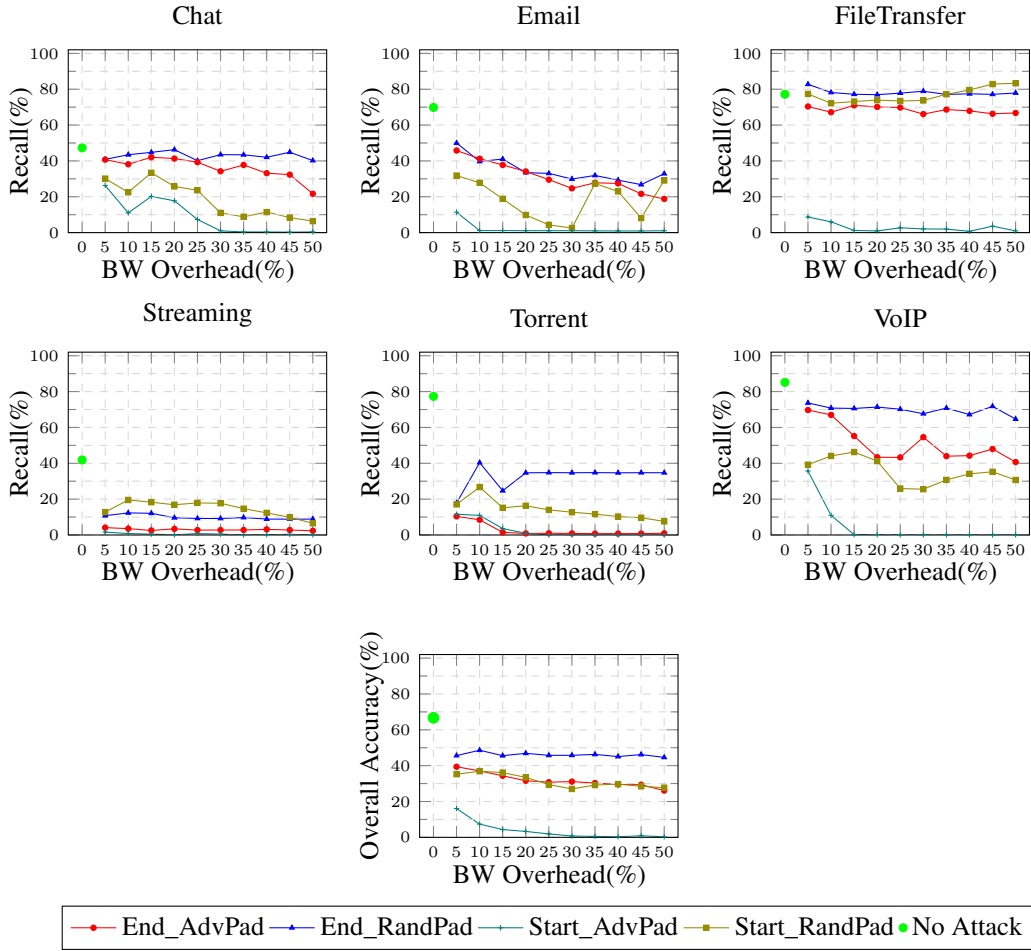


Figure 2: The recall of each class and the overall accuracy of PC-P under different attacks over various sizes of BandWidth (BW) overhead. The legends show the kind of attacks that have been applied to PC-P.

gap between the overall accuracy of the End_AdvPad and the End_AdvPad+Port attack is decreased, which shows that the influence of port attack is reduced by adding more BW overhead. If a random pad injects to the end of the packets payload (End_RandPad), the overall accuracy of PC-HP decreases at most 67.81%, and if this attack joins with the port attack (EndRandPad+Port), the overall accuracy decreases at most 51.08%. Unlike the End_AdvPad attack, by increasing the BW overhead, the gap between the overall accuracy of the End_RandPad and EndRandPad+Port attacks does not decrease, which shows that the End_RandPad can not weaken the influence of port attack. The overall accuracy gaps between the End_AdvPad and End_RandPad attacks and the End_AdvPad+Port, and the End_RandPad+Port attacks show the effectiveness of adversarial pad attack. The End_AdvPad and the End_AdvPad+port attacks reduce the recall for all classes. Nevertheless, these attacks are more effective in chat, email, streaming, and torrent classes rather than file transfer and VoIP classes. In all classes, the End_AdvPad and the End_AdvPad+port attacks reduce recall more compared to the End_RandPad and the End_RandPad+port attacks. By increasing the BW overhead, the distance between the recall of PC-HP under End_RandPad attack and End_RandPad+port attack remain relatively constant for all classes. This distance relates to the sensitivity of PC-HP to the transport-layer port numbers. However, the distance between the recall of PC-HP under the End_AdvPad and the End_AdvPad+port attacks remains relatively small for most of the classes, and in some classes, this distance drops off by adding more BW overhead. These observations show the power of adversarial pad attacks to weaken the influence of the port attack.

The Start_AdvPad attack injects the adversarial pad into the start of the packets payload. This attack reduces the overall accuracy of PC-HP classifier from 88.09% to 28.02% with just 5% BW overhead, and if the BW overhead gets more than 25%, the overall accuracy of PC-HP gets fewer than 5%. The Start_AdvPad+Port attack combines the Start_AdvPad attack with the port attack. This attack decreases the overall accuracy of PC-HP from 88.09% to 18.89% with just 5% BW overhead. The overall accuracies of PC-HP under the Start_AdvPad attack and the

Start_AdvPad+Port attack are very close to each other, which shows that the port attack does not improve the performance of the Start_AdvPad attack. In the Start_RandPad attack, a random pad is injected into the start of the packets payload, and the Start_RandPad+port attack mixes the Start_RandPad with the port attack. There is a significant gap between the overall accuracy of PC-HP under the Start_AdvPad attack and the Start_RandPad attack. Also, there is a large gap between PC-HP overall accuracy under the Start_AdvPad+port attack and the Start_RandPad+port attack. These gaps show the remarkable effectiveness of the adversarial pad at the start of the packets. In all classes, the recall of PC-HP under the Start_AdvPad and the Start_AdvPad+port attacks decreases significantly, and for most classes, after the BW overhead gets more than 20%, the recall of PC-HP gets close to 0%. In all classes with various BW overhead, the distance between PC-HP recall under the Start_AdvPad and the Start_AdvPad+Port attacks is small. However, this distance between the Start_RandPad and the Start_RandPad+Port attacks depends on the class. In some classes, this distance is large, and for others, this distance is small. This observation shows that the port attack improves the performance of the Start_RandPad attack, unlike the Start_AdvPad attack.

The overall accuracies of PC-HP under the End_RandPad and the Start_RandPad attacks are very analogous to each other. Also, PC-HP overall accuracies under the End_RandPad+Port and the Start_RandPad+Port attacks are very close to each other. These observations show injecting a random pad into the end, or into the start of the packets payload has a similar effect on PC-HP overall accuracy. The End_AdvPad and End_AdvPad+Port attacks are more effective than all random pad attacks, which shows adversarial pad at the end of the packets payload are better than random pad at the start of the packets payload. The Start_AdvPad and the Start_AdvPad+Port are the best attacks on PC-HP. These observations show PC-HP is more sensitive to the information at the start of the packet than the information at the end of the packets payload. Also, the results show, as the attack performance improves, the effectiveness of adding the port attack to that attack is decreased. In all classes, the recall of PC-HP under the Start_AdvPad and the Start_AdvPad+Port attacks is reduced more than the End_AdvPad and the End_AdvPad+Port attacks, respectively. Also, in most classes, the performance of random pad attacks is lower than the End_AdvPad and the End_AdvPad+Port attacks. These results show the effectiveness of adversarial pad attacks.

Figure 2 indicates the recall of each class and the overall accuracy of PC-P under proposed attacks for the different magnitudes of BW overhead. The precision and F-score of PC-P under those attacks have been depicted in Figure 9 and Figure 10 in Appendix B. Since transport layer header does not exist in the input of PC-P, the port attack does not work on PC-P. Although the overall accuracy of PC-P is lower than PC-HP, the recall for some classes like VoIP, torrent, file transfer tends to be high. Interestingly, classes that have a high recall in PC-P are more robust against the port attack in PC-HP, which demonstrates that the information in the payload is enough for classifying packets of these classes correctly. The End_AdvPad attack reduces the overall accuracy of PC-P from 66.71% to 39.4% with only 5% BW overhead, and by increasing the BW overhead to 50%, the overall accuracy of PC-P decreases to 26.09%. The overall accuracy of PC-P under the End_RandPad attack is higher than the overall accuracy of PC-P under the End_AdvPad attack, which indicates the effectiveness of the End_AdvPad attack. The performance of the End_AdvPad is variable in the various classes. Although in file transfer and chat classes, the decline of recall of PC-P under the End_AdvPad attack is slight, in most classes, the End_AdvPad attack extremely decreases the recall of PC-P. The decline rate of overall accuracy in End_AdvPad attack over the different values of the BW overhead is relatively low, and by adding more BW overhead, the performance of the End_AdvPad does not increase considerably.

The Start_AdvPad attack significantly decreases the overall accuracy of PC-P, and by 5% and 30% BW overhead, the recall of PC-P reduces to 16.09% and 0.73%, respectively. While the Start_RandPad highly reduces the overall accuracy of PC-P, there is much more drop in the overall accuracy of PC-P under the Start_AdvPad attack rather than Start_RandPad attack. The Start_AdvPad attack indicates the best performance among all attacks on PC-P, and it decreases the recall of each class to less than 3% with just 30% BW overhead. In some classes such as VoIP, email, chat, and file transfer, the recall of PC-P under the Start_RandPad attack is close or lower than recall of PC-P under the End_AdvPad attack. Furthermore, the overall accuracies of PC-P under these two attacks are close to each other. This observation demonstrates PC-P is very sensitive to the information at the start of the packets, so that for PC-P the influence of a random pad at the start of the packets is close or more than the influence of the crafted pad at the end of the packets payload.

5.4 Flow Content Classification

To evaluate the robustness of the flow content classifiers, we propose the adversarial payload (AdvPay) attack. During this attack, a dummy packet that carries adversarial payload is injected into the first n packets of a flow. Also, we propose a random payload (RandPay) attack as the baseline attack to show the effectiveness of the AdvPay attack. In the RandPay attack, a dummy packet that carries a random byte sequence payload is injected into the first n packets of a flow. In this section, first, the dataset and the DL-based classifiers used in FCC are introduced, and then the

Table 4: Flow content classification dataset.

Characte	Imbalanced Dataset		Oversampled Dataset	
	Dataset Quantity	Training Set Quantity	Dataset Quantity	Training Set Quantity
Chat	536	321	1174	959
Email	392	235	1116	959
FileTransfer	1420	852	1527	959
Streaming	1114	668	1405	959
torrent	400	240	1119	959
Voip	1598	959	1598	959
Total	5460	3275	7939	5754

performance of the flow content classifiers, FCC-HP, and FCC-P, is assessed against the AdvPay, the RandPay, and the port attacks.

5.4.1 Flow Content Classification Dataset

The dataset needs to be normalized for flow content classification. Similar to packet classification, the decimal value of each byte is divided by 255 to normalize the byte sequence of packets between zero and one, and then, zero pad is added to the end of the packets until their length reaches to *MaxPktSize*. Afterward, the byte sequences of the first n packets of a flow which have at least one byte payload are concatenated together, and this new sequence is called flow byte sequence. To clean the dataset from background flows, we only choose flows with at least 1000 bytes of payload and at least three packets containing the payload.

Since the dataset is highly imbalanced, we use oversampling to increase the number of samples in classes that have fewer data. We consider 60% of the dataset as the training set, 20% of it as the validation set, and 20% of it as the test set. In oversampling, certain numbers of data are sampled from classes that have fewer samples and are replicated to the dataset until their data numbers reach the class that has the most number of data. Table 4 indicates the number of samples in each class before and after oversampling. It is notable that we only increase the amount of data in the training set, and before and after oversampling, the number of samples in the validation and the test sets are the same.

5.4.2 Flow Content Classifiers Setup

A 1D-CNN is used to classify flows using the byte sequence of the content of flows. Given our Computational resource, more than 150 1D-CNN with various architectures and hyperparameters have been explored to find the best classifier for FCC. Eventually, the classifier with higher accuracy on the validation set has been chosen. The architecture and hyperparameters of the selected classifier are reported in Table 8 in Appendix A.

To determine the number of packets in the byte sequence of each flow, we have examined the different numbers of packets in the flow byte sequence. The results are presented in Table 10 in Appendix A. We have two criteria to choose the number of packets in flow byte sequence: (i) the classifier should have high performance on it, and (ii) for enforcing online policies on network flows, number of packets should be as few as possible. Based on experiments, we choose ten packets of each flow to be in each flow byte sequence. If a flow has more than ten packets, we only consider the byte sequence of the first ten packets of the flow, and if a flow has less than ten packets, we add zero pad at the end of it.

We train two classifiers, FCC-Hp and FCC-p. In FCC-HP, packets residing in the flow byte sequence have the transport-layer header and the payload, and in FCC-P, Packets only have the payload. The accuracies of FCC-HP and FCC-P are 81.52% and 80.6%, respectively. Other performance metrics of these classifiers are presented in Table 5. The results demonstrate that the influence of the transport layer header on FCC is low, and even in some classes, the performance of FCC-P is better than FCC-HP. The performance of classifiers is comparable to the study [25], which has classified flows using the content of packets on the "ISCXVPN2016" dataset.

5.4.3 Flow Content Classifiers Robustness Evaluation

For evaluating the robustness of Flow content classifiers, the AdvPay, the RandPay, and the port attacks have been applied to these classifiers. The AdvPay attack has been run for 1000 iterations with *batch_size*=128 and $\epsilon = 0.001$. The dummy packet is injected after the first packet from the source (e.g., client) to the destination (e.g., server). The RandPay attack has been conducted 50 times, and the average results are reported in this section.

Table 5: Performance metrics of the flow content classifiers, FCC-HP, and FCC-P.

Character	FCC-HP			FCC-P		
	Precision(%)	Recall(%)	F-score(%)	Precision(%)	Recall(%)	F-score(%)
Chat	73.26	58.88	65.29	74.39	57.01	64.55
Email	89.04	82.28	85.53	85.37	88.61	86.96
FileTransfer	85.17	86.97	86.06	90.23	84.51	87.28
Streaming	79.82	81.61	80.71	74.69	82.06	78.25
Torrent	98.7	95.00	96.81	97.47	96.25	96.86
VoIP	76.11	80.62	78.30	73.75	78.12	75.87

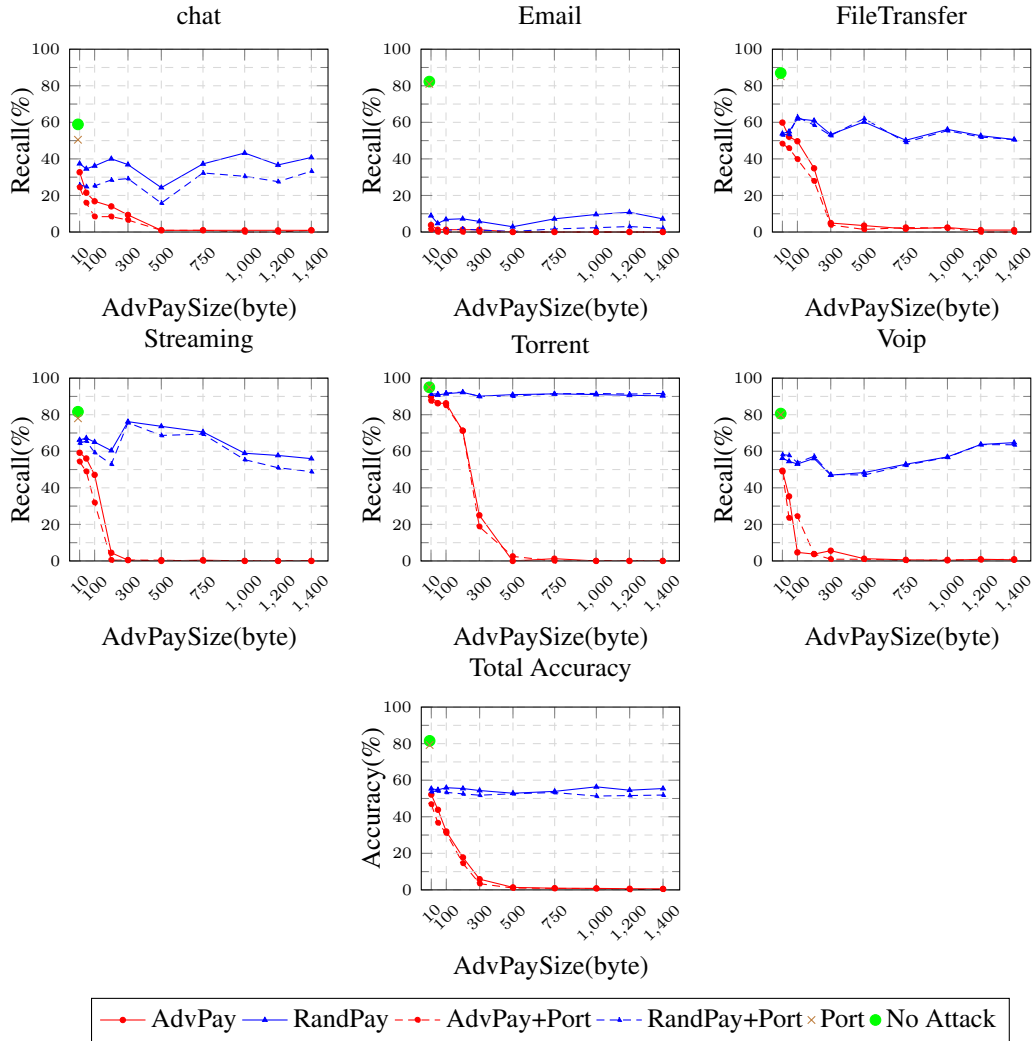


Figure 3: The recall of each class and the overall accuracy of FCC-HP under different attacks over various sizes of the adversarial payload. The legends show the kind of attacks that have been applied to FCC-HP.

Figure 3 shows the recall for each class and the overall accuracy of FCC-HP under the port, the AdvPay, and the RandPay attacks over various sizes of the adversarial payload. The precision and F-score of FCC-HP under these attacks are presented in Figure 11 and Figure 12 in Appendix C. The overall accuracy of FCC-HP under port attack decreases from 81.52% to 79.23%, which shows FCC-HP does not rely too much on the information in the transport layer port. Chat and streaming classes are the only two classes that the port attack reduces the recall of FCC-HP on them; however, the size of this reduction is small.

In the AdvPay attack, first, Algorithm 2 generates a universal adversarial perturbation on flows belonging to the validation set with the desired size. Afterward, for each flow in the test set, this perturbation is injected into the payload of a dummy packet, which lies after the first packet that is moving from the source to the destination. For example, Algorithm 2 generates a universal adversarial perturbation with size 100 on the chat flows in the validation set. Then for each flow of chat class in the test set, this perturbation is injected into the payload of a dummy packet, which exists after the first packet from the source to the destination on chat flows in the test set. This attack decreases the overall accuracy of FCC-HP from 81.52% to 52.15% with just ten bytes of adversarial payload. If the size of the adversarial payload is increased to 500 bytes, the overall accuracy of FCC-HP drops to 1.37%. The AdvPay+Port attack combines AdvPay attack with the port attack. It increases the performance of the AdvPay attack a little bit, and by 10 and 500 bytes adversarial payload, the overall accuracy of FCC-HP drops down to 46.75% and 1.01%, respectively. The AdvPay and the AdvPay+Port attacks are effective in all classes. With 500 bytes of adversarial payload, the recall for all classes under the AdvPay and the AdvPay+Port attacks drops to less than 3.52% and 1.41%, respectively. The RandPay attack injects a dummy packet with random byte sequence payload after the first packet from the source to the destination in a flow. Although the performance of the RandPay attack is good, and the recall of FCC-HP under this attack decreases to 55.35%, the AdvPay attack has much better performance than this attack. When the size of the adversarial payload is small, the distance between the overall accuracy of FCC-HP under the RandPay and the AdvPay is relatively small. However, when the payload size of the dummy packet gets increased, this distance becomes more and more, which demonstrates the effectiveness of the AdvPay attack. The RandPay+Port attack combines the RandPay attack with the port attack. The overall performance of the RandPay+Port attack is very close to the RandPay attack. Unlike the AdvPay attack, by increasing the adversarial payload size, the overall accuracy of FCC-HP under the RandPay and the RandPay+Port attacks remains relatively fixed. However, FCC-HP overall accuracy under the AdvPay and the AdvPay+Port attacks gets better by increasing the size of the adversarial payload. The performance of the RandPay and the RandPay+Port attack are different in various classes. There is a significant decline in the recall of fcc-HP under these attacks over email class, also for other classes including chat, file transfer, VoIP, and streaming, the decline is fairly large. However, the performance of these attacks on the torrent class is weak.

Figure 4 indicates the recall and overall accuracy of FCC-P under the AdvPay and the RandPay attacks over various sizes of the adversarial payload. The precision and F-score of FCC-P under these attacks are depicted in Figure 13 and Figure 14 in Appendix C. Because of the lack of transport layer header in the input of FCC-P, the port attack is not effective. With just ten bytes adversarial payload, the overall accuracy of FCC-P reduces from 80.6% to 46.94%, and if the size of the adversarial pad increases to 1000 bytes, the overall accuracy of FCC-P decreases to 1.56%. By increasing the adversarial payload size over ten bytes, the decline rate of overall accuracy under the AdvPay attack is high at first. Then, by increasing the size of the adversarial payload, it gets decreased until converges to zero after 1000 bytes adversarial payload. This pattern of reduction repeats for recall of FCC-P under the AdvPay attack for all classes. Except for torrent class, the recall for all classes under the AdvPay attack drops off to almost 0% with 1000 or fewer bytes adversarial payload. The recall of torrent class decreases to 0% with 1400 bytes adversarial payload.

The RandPay attack reduces the overall accuracy of FCC-P from 80.6% to 58.55% with only ten bytes of random payload, and unlike AdvPay attack, by increasing the size of the random payload, the performance of RandPay attack does not improve very much. This observation repeats on FCC-P recall under the RandPay attack over all classes, which demonstrates the effectiveness of the AdvPay attack on FCC-P.

Although FCC-P has almost 1% less accuracy than FCC-HP, the results in Figure 3 and Figure 4 indicate FCC-P is slightly more robust than FCC-HP, and for reducing the performance of FCC-P, an attacker needs to increase the size of the adversarial payload. The performances of the RandPay attack on FCC-HP and FCC-P are almost the same, which shows that these classifiers have quite identical robustness against the RandPay attack.

5.5 Flow Time Series Classification

In this section, we evaluate the robustness of the flow time series classifiers against the AdvBurst attack. First, we need to build two versions of this classifier. In the first version, the classifier uses packets size, and in the second version, the classifier uses the Inter-arrival times between packets to classify flows. Later, we apply the AdvBurst attack on these classifiers to evaluate their robustness. To evaluate the effectiveness of the AdvBurst attack, we also conduct the RandBurst attack on these classifiers. The AdvBurst attack must have better performance than the RandBurst attack. In the RandBurst attack, the statistical features of dummy packets in the adversarial burst is randomly perturbed. In this section, first, the dataset and the DL-based classifiers used in FTSC are introduced, and then the performance of the flow time series classifiers, FTSC-PS, and FTSC-IAT, is assessed against the AdvBurst, and the RandBurstattacks.

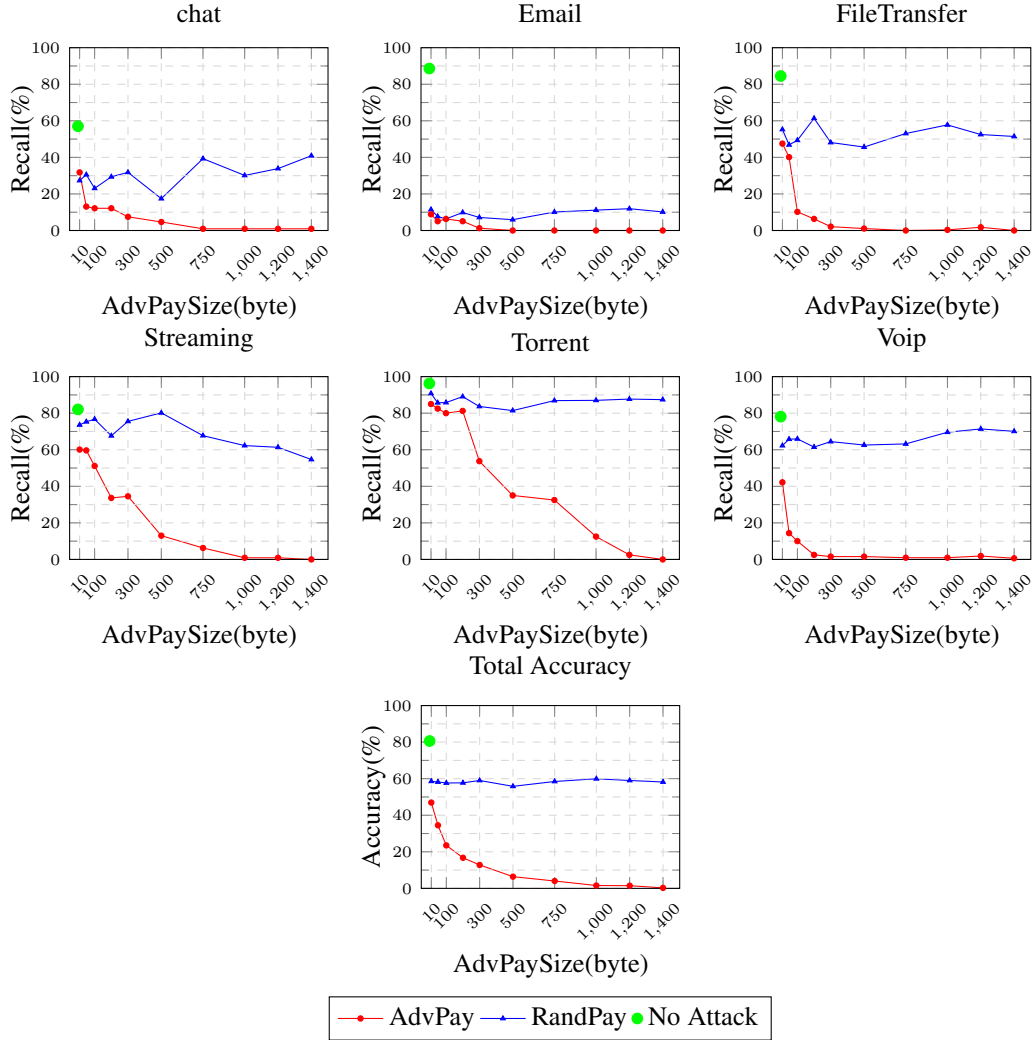


Figure 4: The recall of each class and the overall accuracy of FCC-P under different attacks over various sizes of the adversarial payload. The legends show the kind of attacks that have been applied to FCC-P.

5.5.1 Flow Time Series Classification Dataset

The dataset of FTSC consists of time series of inter-arrival times between packets, packets size of each flow. The cleaning process on the "ISCXVPN2016" dataset is precisely like FCC cleaning process and, the number of samples in each class is very close to FCC dataset (Table 4). We remove flows that have less than three packets and 1000 bytes of payload. Also, we use oversampling to increase the number of samples in the classes that have fewer samples. The domain of packet size is between the minimum header size and $MaxPktSize$. The packets size is first normalized by standard normalization (Equation 29), and later the minimum of normalized data is added to them which makes normalized data positive. Finally, by dividing normalized data in the maximum of them, the domain of normalized data is limited between zero and one. In the next step, the normalized packet size vector of each flow is multiplied to the vector of the direction sign (Equation 6).

$$Normalized\ Packet\ Size = \frac{PacketSize - \mu_{PktSize}}{Std_{PktSize}} \quad (29)$$

where $\mu_{PktSize}$, and $Std_{PktSize}$ indicate mean and standard deviation of packets size, respectively. The domain of inter-arrival time is between zero microseconds and the longest flow timeout. The flow timeout is configurable, and in our system, the longest flow timeout is 180 seconds. To prepare data, first, the log normalization (Equation 30) is used to normalize inter-arrival time data, and afterward, the sign of packets is multiplied in the direction to them.

$$Normalized\ InterArrivalTime = 2 \times \log_{IAT_{max}}^{(InterArrivalTime+1)} \quad (30)$$

Table 6: Performance metrics of the flow time series classifiers, FTSC-PS, and FTSC-IAT.

Character	FTSC-PS			FTSC-IAT		
	Precision(%)	Recall(%)	F-score(%)	Precision(%)	Recall(%)	F-score(%)
Chat	58.25	58.25	58.25	65.22	58.25	61.54
Email	92.21	89.89	91.02	85.54	89.87	87.65
FileTransfer	80.00	76.60	78.26	80.95	78.37	79.64
Streaming	78.28	71.10	74.52	75.00	70.18	72.51
Torrent	88.24	93.75	90.91	90.24	92.50	91.36
VoIP	70.85	77.39	73.98	71.39	77.81	74.46

where IAT_{max} is the maximum of inter-arrival times data.

5.5.2 Flow Time Series Classifiers Setup

We have used a 1D-CCN to classify flow time series and have explored more than 150 different architectures and hyperparameters to build the final flow time series classifier. The architecture and hyperparameters of selected 1D-CNN are presented in Table 9 in Appendix A. To choose the number of packets in each flow time series, we have investigated the different numbers of packets in the time series. The results are in Table 10 in Appendix A. Based on experiments, we choose 100 packets of each flow to be in the flow time series. If a flow has more than 100 packets, the statistical features of the first 100 packets of the flow are only put in that flow time series, and if a flow has less than 100 packets, zero pad is added to the end of it. The accuracies of FTSC-PS and FTSC-IAT with 100 packets in each flow time series are 76.21% and 76.51%, respectively, and other performance metrics of these classifiers are reported on Table 6. Based on our experiments, FTSC-IAT has a little bit better performance than FTSC-PS. Our results are relatively close to past studies that use flow time-series to classify ISCXVPN2016 dataset [10, 15]. In [10, 15], the cleaning process and the number of data in each class have not been reported, and we can not tell the reason for this difference.

5.5.3 Flow Time Series Classifiers Robustness Evaluation

For evaluating the robustness of flow time series classifiers, AdvBurst and the RandBurst attacks have been applied to these classifiers. AdvBurst attack has run for 2000 iterations with $batch_siz=128$ and $\epsilon = 0.01$. Since the domain of IAT is vast, we need to restrict the inter-arrival time domain of dummy packets. The domain of IAT is between 0 and 180 seconds, with microsecond granularity. A challenging issue when the domain of dummy packets IAT equals the domain of IAT in the dataset. The AdvBurst attack can impose high time overhead on a flow. For instance, the AdvBurst attack can add 1800 seconds to the duration of a flow with just ten dummy packets, which is unacceptable. To overcome this challenge, we limit the domain of dummy packets IAT between 0.001 and 0.1 seconds. We apply this limit using the clip function in the adversarial burst algorithm (see Algorithm 3).

In the AdvBurst attack, first, Algorithm 3 generates a universal adversarial perturbation with the desired number of dummy packets on the flows of a specific character in the validation set. Afterward, this perturbation is used as the statistical feature of dummy packets, and dummy packets are appended to the end of the selected bursts of that character flows in the test set. For example, at the first step, Algorithm 3 makes a universal adversarial perturbation with size three for three dummy packets on the email flows in the validation set. Afterward, this perturbation is used as the statistical feature of the dummy packets, which are appended to the end of the selected bursts of the email flow in the test set, and the robustness of the classifiers is evaluated against these flows. The RandBurst attack has been conducted 50 times, and the average results are reported in this section.

To attack FTSC-PS by the AdvBurst attack, we choose the first burst from the source to the destination as the selected burst in all flows, and dummy packets with the adversarial statistical feature are appended to the end of these bursts. Figure 5 shows the recall for each class and the overall accuracy of FTSC-PS under the AdvBurst and the RandBurst attacks over different numbers of dummy packets, which have s been added to the end of the first burst from the source to the destination. The precision and F-score of FTSC-PS under these attacks are presented in Figure 15 and Figure 16 in Appendix D. With just one dummy packet, the AdvBurst attack decreases the overall accuracy of FTSC-PS from 76.21% to 49.63%, and by adding more dummy packets at the end of the selected burst, the overall accuracy more decreases. As an example, with 7 and 15 dummy packets, the overall accuracy of FTSC-PS under the AdvBurst attack decreases to 20.07% and 11.06%, respectively. The RandBurst attack appends dummy packets with random statistical features at the end of the selected burst. This attack reduces the overall accuracy of FTSC-PS from 76.21% to 56.13%, and by increasing the number of dummy packets, the experiments show that the overall accuracy of FTSC-PS decreases further. For example, the overall accuracy of FTSC-PS under this attack decreases to 41.26%

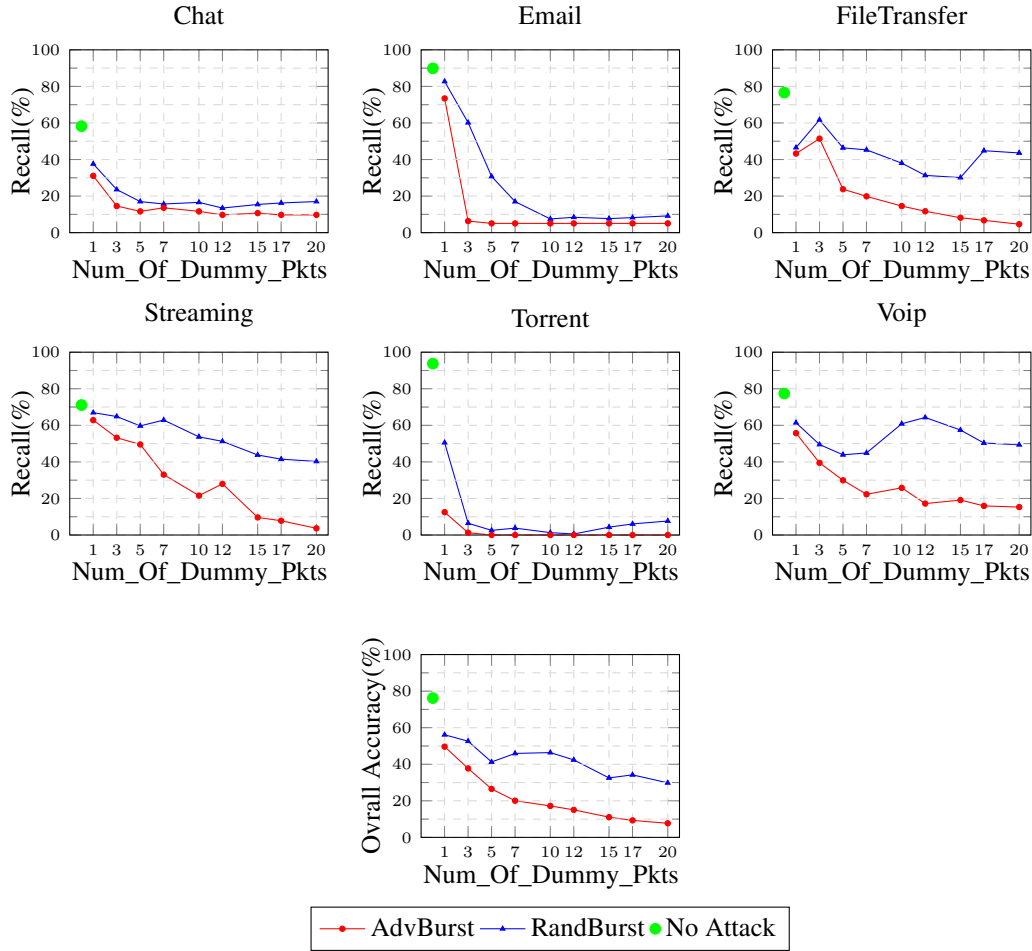


Figure 5: The recall of each class and the overall accuracy of FTSC-PS under different attacks over the various number of dummy packets. The legends show the kind of attacks that have been applied to FTSC-PS.

and 32.53% with 5 and 15 dummy packets, respectively. The distance between the overall accuracy of FTSC under the AdvBurst and the RandBurst attack rises by adding more dummy packets to the adversarial burst, which shows that doing so will improve the performance of the AdvBurst attack more than the RandBurst attack. In chat, email, and torrent classes, the recall of FTSC-PS under the AdvBurst attack drops to less than 11.65% using just five dummy packets. Also, the RandBurst attack shows excellent performance in these classes. Although the AdvBurst attack has better performance on these classes, results show these classes are highly vulnerable to little manipulation in the size of dummy packets, and even dummy packets with random packet sizes can highly decrease the recall for these classes. In contrast, although the performances of the AdvBurst attack in file transfer, streaming, and VoIP classes, are not as fine as those classes, the distance between the recall of FTSC-PS under the AdvBurst and the RandBurst attacks is large. This observation indicates the effectiveness of the AdvBurst attack in these classes.

To carry out the AdvBurst attack on FTSC-IAT, we consider the first burst from the destination to the source in a flow as the selected burst for making adversarial burst and dummy packets are appended to the end of it. As mentioned earlier in this section, the minimum and maximum inter-arrival time that a dummy packet adds to a flow are 0.001 and 0.1 seconds, respectively. For example, by appending ten dummy packets to the adversarial burst, the duration of flow is increased by one second. Figure 6 shows the recall of each class and the overall accuracy of FTSC-IAT under the AdvBurst and the RandBurst attacks. The precision and F-score of FTSC-PS under these attacks are depicted in Figure 17 and Figure 18 in Appendix D. The overall accuracy of FTSC-IAT under the AdvBurst attack reduces from 76.51% to 58.81%, with only one dummy packet. By increasing the number of dummy packets, the overall accuracy under the AdvBurst attack is further decreased. As an example, with 7 and 20 dummy packets, the overall accuracy of FTSC-IAT under the AdvBurst attack reduces to 31.97% and 20.97%, respectively. The RandBurst attack decreases the overall accuracy of FTSC-IAT to 60.11% with just one dummy packet. Similar to the AdvBurst attack, the overall

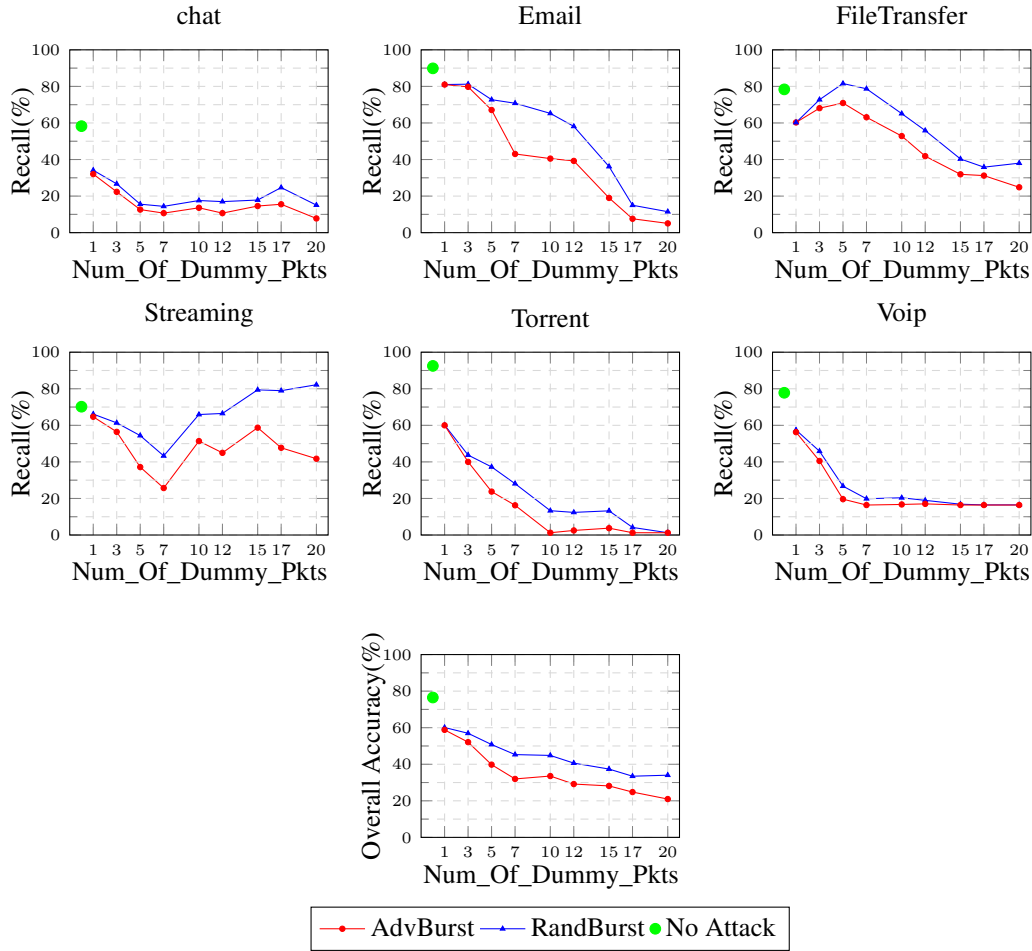


Figure 6: The recall of each class and the overall accuracy of FTSC-IAT under different attacks over the various number of dummy packets. The legends show the kind of attacks that have been applied to FTSC-IAT.

accuracy gets increased by raising the number of dummy packets. Although the performance of the AdvBurst attack on FTSC-IAT is fine enough and the decline in the overall accuracy is notable, the gap between the overall accuracy of FTSC-IAT under the AdvBurst and the RandBurst attacks is relatively small. We think the effectiveness of AdvBurst attack has decreased because of the domain of inter-arrival time has been limited between 0.001 and 0.1 seconds, and this domain is remarkably shorter than the real domain of inter-arrival time in the dataset.

The AdvBurst attack reduces the recall for all classes. However, its performance is various in different classes. The AdvBurst attack highly decreases the recall of FTSC-IAT for some classes such as chat, torrent, and VoIP, and with just seven dummy packets, the recall of these classes becomes less than 16.4%. The AdvBurst attack needs more dummy packets to highly decrease the recall of FTSC-IAT for email and file transfer classes. By increasing the number of dummy packets, the recall of streaming class under the AdvBurst attack has a strange behavior. The recall tends to decrease continuously until the seventh dummy packet is added, and after that, it begins to rise. We think the reason for this behavior is that the size of the burst heading from destination to source is often large in streaming class, and by increasing the number of dummy packets, the size of the adversarial burst gets increased, and as a consequence, FTSC-PS recognizes these flows as the streaming.

6 Conclusion

In this paper, the robustness of DL-based network traffic classifiers against Adversarial Network Traffic (ANT) has been evaluated. Based on the literature, we considered three input space categories in DL-based network traffic classification, which include PC, FCC, and FTSC. Based on these categories, we proposed three new attacks to make ANT. The AdvPad attack weakens the performance of PC-P and PC-HP with low bandwidth overhead, and by increasing

the size of bandwidth overhead, the performance of classifiers are more reduced. The results demonstrated injecting the adversarial pad at the start of packets payload decreases the performance of classifiers more than the end of the payload of packets. The robustnesses of PC-HP and PC-P are low and almost equal. However, PC-HP showed better performance in a benign environment. The AdvPay attack has reduced the performance of flow content classifiers FCC-HP and FCC-P, and by increasing the size of the adversarial payload, the performances of classifiers are further decreased. The robustnesses of FCC-HP and FCC-P are close to each other, but FCC-P is more robust for some classes. By and large, the robustnesses of flow content classifiers are very low, and by just 500 bytes of adversarial payload, the recall of most classes comes close to zero. The AdvBurst attack has reduced the performance of flow time series classifiers. The AdvBurst attack is very simple and highly decreases the performance of FTSC-PS and FTSC-IAT by just a few dummy packets with crafted statistical features. FTSC-IAT is rather more robust than FTSC-PS. Although the proposed attacks are very simple, the performances of classifiers have highly decreased, which demonstrates that DL-based network traffic classifiers have very low robustness. The Robustness of DL-based network traffic classifiers is a critical issue, and by continuing researches in this area, we aim to increase the robustness of these classifiers.

7 Acknowledgement

The authors would like to express their very great appreciation to Hamid Reza Tajali for his valuable discussions, reviews, and feedback.

References

- [1] Alberto Dainotti, Antonio Pescapè, and Kimberly C. Claffy. Issues and future directions in traffic classification. *IEEE Network*, 26(1):35–40, 2012.
- [2] Fannia Pacheco, Ernesto Exposito, Mathieu Gineste, Cédric Baudoin, and José Aguilar. Towards the deployment of machine learning solutions in network traffic classification: A systematic survey. *IEEE Communications Surveys and Tutorials*, 21(2):1988–2014, 2019.
- [3] Internet assigned numbers authority. <https://www.iana.org/>. Accessed: 2020-02-27.
- [4] Yaxuan Qi, Lianghong Xu, Baohua Yang, Yibo Xue, and Jun Li. Packet classification algorithms: From theory to practice. In *INFOCOM 2009. 28th IEEE International Conference on Computer Communications, Joint Conference of the IEEE Computer and Communications Societies, 19-25 April 2009, Rio de Janeiro, Brazil*, pages 648–656, 2009.
- [5] Maurizio Dusi, Francesco Gringoli, and Luca Salgarelli. Quantifying the accuracy of the ground truth associated with internet traffic traces. *Comput. Networks*, 55(5):1158–1167, 2011.
- [6] Alex Krizhevsky, Ilya Sutskever, and Geoffrey E. Hinton. Imagenet classification with deep convolutional neural networks. In *Advances in Neural Information Processing Systems 25: 26th Annual Conference on Neural Information Processing Systems 2012. Proceedings of a meeting held December 3-6, 2012, Lake Tahoe, Nevada, United States*, pages 1106–1114, 2012.
- [7] Deep neural networks for acoustic modeling in speech recognition: The shared views of four research groups. *IEEE Signal Process. Mag.*, 29(6):82–97, 2012.
- [8] David Silver, Aja Huang, Chris J. Maddison, Arthur Guez, Laurent Sifre, George van den Driessche, Julian Schrittwieser, Ioannis Antonoglou, Vedavyas Panneershelvam, Marc Lanctot, Sander Dieleman, Dominik Grewe, John Nham, Nal Kalchbrenner, Ilya Sutskever, Timothy P. Lillicrap, Madeleine Leach, Koray Kavukcuoglu, Thore Graepel, and Demis Hassabis. Mastering the game of go with deep neural networks and tree search. *Nature*, 529(7587):484–489, 2016.
- [9] Manuel López Martín, Belén Carro, Antonio Sánchez-Esguevillas, and Jaime Lloret. Network traffic classifier with convolutional and recurrent neural networks for internet of things. *IEEE Access*, 5:18042–18050, 2017.
- [10] Julian Andres Caicedo-Muñoz, Agapito Ledezma Espino, Juan Carlos Corrales, and Álvaro Rendón Gallón. Qos-classifier for VPN and non-vpn traffic based on time-related features. *Computer Networks*, 144:271–279, 2018.
- [11] Giuseppe Aceto, Domenico Ciuonzo, Antonio Montieri, and Antonio Pescapè. Mobile encrypted traffic classification using deep learning: Experimental evaluation, lessons learned, and challenges. *IEEE Trans. Network and Service Management*, 16(2):445–458, 2019.
- [12] Payap Sirinam, Mohsen Imani, Marc Juárez, and Matthew Wright. Deep fingerprinting: Undermining website fingerprinting defenses with deep learning. In *Proceedings of the 2018 ACM SIGSAC Conference on Computer and Communications Security, CCS 2018, Toronto, ON, Canada, October 15-19, 2018*, pages 1928–1943, 2018.

- [13] Vera Rimmer, Davy Preuveneers, Marc Juárez, Tom van Goethem, and Wouter Joosen. Automated website fingerprinting through deep learning. In *25th Annual Network and Distributed System Security Symposium, NDSS 2018, San Diego, California, USA, February 18-21, 2018*, 2018.
- [14] Mohammad Lotfollahi, Mahdi Jafari Siavoshani, Ramin Shirali Hossein Zade, and Mohammadsadeh Saberian. Deep packet: a novel approach for encrypted traffic classification using deep learning. *Soft Comput.*, 24(3):1999–2012, 2020.
- [15] Gerard Draper-Gil, Arash Habibi Lashkari, Mohammad Saiful Islam Mamun, and Ali A. Ghorbani. Characterization of encrypted and VPN traffic using time-related features. In *Proceedings of the 2nd International Conference on Information Systems Security and Privacy, ICISSP 2016, Rome, Italy, February 19-21, 2016*, pages 407–414, 2016.
- [16] Mohammad Saiful Islam Mamun, Ali A. Ghorbani, and Natalia Stakhanova. An entropy based encrypted traffic classifier. In *Information and Communications Security - 17th International Conference, ICICS 2015, Beijing, China, December 9-11, 2015, Revised Selected Papers*, pages 282–294, 2015.
- [17] Nicolas Papernot, Patrick D. McDaniel, Arunesh Sinha, and Michael P. Wellman. Sok: Security and privacy in machine learning. In *2018 IEEE European Symposium on Security and Privacy, EuroS&P 2018, London, United Kingdom, April 24-26, 2018*, pages 399–414, 2018.
- [18] Christian Szegedy, Wojciech Zaremba, Ilya Sutskever, Joan Bruna, Dumitru Erhan, Ian J. Goodfellow, and Rob Fergus. Intriguing properties of neural networks. In *2nd International Conference on Learning Representations, ICLR 2014, Banff, AB, Canada, April 14-16, 2014, Conference Track Proceedings*, 2014.
- [19] Nicholas Carlini and David A. Wagner. Towards evaluating the robustness of neural networks. In *2017 IEEE Symposium on Security and Privacy, SP 2017, San Jose, CA, USA, May 22-26, 2017*, pages 39–57, 2017.
- [20] Ian J. Goodfellow, Jonathon Shlens, and Christian Szegedy. Explaining and harnessing adversarial examples. In *3rd International Conference on Learning Representations, ICLR 2015, San Diego, CA, USA, May 7-9, 2015, Conference Track Proceedings*, 2015.
- [21] Seyed-Mohsen Moosavi-Dezfooli, Alhussein Fawzi, and Pascal Frossard. Deepfool: A simple and accurate method to fool deep neural networks. In *2016 IEEE Conference on Computer Vision and Pattern Recognition, CVPR 2016, Las Vegas, NV, USA, June 27-30, 2016*, pages 2574–2582, 2016.
- [22] Nicolas Papernot, Patrick D. McDaniel, Somesh Jha, Matt Fredrikson, Z. Berkay Celik, and Ananthram Swami. The limitations of deep learning in adversarial settings. In *IEEE European Symposium on Security and Privacy, EuroS&P 2016, Saarbrücken, Germany, March 21-24, 2016*, pages 372–387, 2016.
- [23] Nicolas Papernot, Patrick D. McDaniel, and Ian J. Goodfellow. Transferability in machine learning: from phenomena to black-box attacks using adversarial samples. *CoRR*, abs/1605.07277, 2016.
- [24] Seyed-Mohsen Moosavi-Dezfooli, Alhussein Fawzi, Omar Fawzi, and Pascal Frossard. Universal adversarial perturbations. In *2017 IEEE Conference on Computer Vision and Pattern Recognition, CVPR 2017, Honolulu, HI, USA, July 21-26, 2017*, pages 86–94, 2017.
- [25] Wei Wang, Ming Zhu, Jinlin Wang, Xuewen Zeng, and Zhongzhen Yang. End-to-end encrypted traffic classification with one-dimensional convolution neural networks. In *2017 IEEE International Conference on Intelligence and Security Informatics, ISI 2017, Beijing, China, July 22-24, 2017*, pages 43–48, 2017.
- [26] Ian Goodfellow, Yoshua Bengio, and Aaron Courville. *Deep Learning*. MIT Press, 2016. <http://www.deeplearningbook.org>.
- [27] Alexey Kurakin, Ian J. Goodfellow, and Samy Bengio. Adversarial examples in the physical world. In *5th International Conference on Learning Representations, ICLR 2017, Toulon, France, April 24-26, 2017, Workshop Track Proceedings*, 2017.
- [28] Pan Wang, Feng Ye, Xuejiao Chen, and Yi Qian. Datanet: Deep learning based encrypted network traffic classification in SDN home gateway. *IEEE Access*, 6:55380–55391, 2018.
- [29] Zhanyi Wang. The applications of deep learning on traffic identification. *BlackHat USA*, 24, 2015.
- [30] Wei Wang, Ming Zhu, Xuewen Zeng, Xiaozhou Ye, and Yiqiang Sheng. Malware traffic classification using convolutional neural network for representation learning. In *2017 International Conference on Information Networking, ICOIN 2017, Da Nang, Vietnam, January 11-13, 2017*, pages 712–717, 2017.
- [31] Vincent F. Taylor, Riccardo Spolaor, Mauro Conti, and Ivan Martinovic. Robust smartphone app identification via encrypted network traffic analysis. *IEEE Trans. Information Forensics and Security*, 13(1):63–78, 2018.

- [32] Vincent F. Taylor, Riccardo Spolaor, Mauro Conti, and Ivan Martinovic. Appscanner: Automatic fingerprinting of smartphone apps from encrypted network traffic. In *IEEE European Symposium on Security and Privacy, EuroS&P 2016, Saarbrücken, Germany, March 21-24, 2016*, pages 439–454, 2016.
- [33] Kota Abe and Shigeki Goto. Fingerprinting attack on tor anonymity using deep learning. *Proceedings of the Asia-Pacific Advanced Network*, 42:15–20, 2016.
- [34] Shahbaz Rezaei and Xin Liu. How to achieve high classification accuracy with just a few labels: A semi-supervised approach using sampled packets. *CoRR*, abs/1812.09761, 2018.
- [35] Joseph Kampeas, Asaf Cohen, and Omer Gurewitz. Traffic classification based on zero-length packets. *IEEE Trans. Network and Service Management*, 15(3):1049–1062, 2018.

Appendices

A Architecture and hyperparameters of different classifiers

Table 7: The architecture (A) and hyperparameters (B) of 1D-CNN packet classifiers, PC-HP, and PC-P.

(A)			(B)	
#	Layer	Parameters	Hyperparameter	Value
1	1D-Convolution	Number of filters: 256, Filter size: 4, Strides: 2	Optimizer	Adamax
2	Batch normalization	-	Learning rate	0.0005
3	Relu	-	Batch size	128
4	1D-Convolution	Number of filters: 128, Filter size: 8, Stride: 2	Epoch number	1000
5	Batch Normalization	-	Validation metric	Accuracy
6	Relu	-	DL framework	Tensorflow & Keras
7	1D-Max Polling	Filter size: 2, Strides: 1		
8	Dense	Size: 256		
9	Batch normalization	-		
10	Relu	-		
11	Dropout	Rate: 0.1		
12	Dense	Size: 128		
13	Batch normalization	-		
14	Relu	-		
15	Dropout	Rate: 0.1		
16	Dense	Size: 6		
17	Softmax	-		

Table 8: The architecture (A) and hyperparameters (B) of 1D-CNN flow content classifiers, FCC-HP, and FCC-P.

(A)						(B)	
#	Layer	Parameters	#	Layer	Parameters	Hyperparameter	Value
1	1D-convolution	Number of filters: 32 Filter size: 4 Strides: 1	17	Dense	Size: 512	Optimizer	Adamax
2	Elu	Alpha: 1.0	18	Batch normalization	-	Learning rate	0.0005
3	Batch normalization	-	19	Relu	-	Batch size	128
4	1D-Max pooling	Filter size: 8 Strides: 2	20	Dropout	Rate: 0.05	Epoch number	1000
5	1D-convolution	Number of filters: 64 Filter size: 4 Strides: 1	21	Dense	Size: 512	Validation metric	Accuracy
6	Elu	Alpha: 1.0	22	Batch normalization	-	DL framework	Tensorflow & Keras
7	Batch normalization	-	23	Relu	-		
8	1D-Max pooling	Filter size: 8 Strides: 2	24	Dropout	Rate: 0.05		
9	1D-convolution	Number of filters: 128 Filter size: 8 Strides: 1	25	Dense	Size: 6		
10	Elu	Alpha: 1.0	26	Softmax	-		
11	Batch normalization	-					
12	1D-Max pooling	Filter size: 8 Strides: 2					
13	1D-convolution	Number of filters: 256 Filter size: 8 Strides: 1					
14	Elu	Alpha: 1.0					
15	Batch normalization	-					
16	1D-Max pooling	Filter size: 8 Strides: 2					

Adversarial Network Traffic:
Toward Evaluating the Robustness of Deep Learning Based Network Traffic Classification

Table 9: The architecture (A) and hyperparameters (B) of 1D-CNN flow time series classifiers, FTSC-PS, and FTSC-IAT.

(A)					
#	Layer	Parameters	#	Layer	Parameters
1	1D-Convolution	Number of filters: 128, Filter size: 16, Strides: 1	22	1D-Convolution	Number of filters: 256, Filter size: 4, Strides: 1
2	Elu	Alpha: 1.0	23	Elu	Alpha: 1.0
3	Batch normalization	-	24	Batch normalization	-
4	1D-Convolution	Number of filters: 128, Filter size: 16, Stride: 1	25	1D-Convolution	Number of filters: 256, Filter size: 4, Strides: 1
5	Elu	Alpha: 1.0	26	Elu	Alpha: 1.0
6	Batch Normalization	-	27	Batch Normalization	-
7	1D-Max Polling	Filter size: 4, Strides: 2	28	1D-Max Polling	Filter size: 4, Strides: 2
8	1D-Convolution	Number of filters: 128, Filter size: 8, Strides: 1	29	Dense	Size: 1024
9	Elu	Alpha: 1.0	30	Batch normalization	-
10	Batch normalization	-	31	Relu	-
11	1D-Convolution	Number of filters: 128, Filter size: 8, Strides: 1	32	Dropout	Rate: 0.05
12	Elu	Alpha: 1.0	33	Dense	Size: 512
13	Batch Normalization	-	34	Batch normalization	-
14	1D-Max Polling	Filter size: 4, Strides: 2	35	Relu	-
15	1D-Convolution	Number of filters: 128, Filter size: 4, Strides: 1	36	Dropout	Rate: 0.05
16	Elu	Alpha: 1.0	37	Dense	Size: 512
17	Batch normalization	-	38	Batch normalization	-
18	1D-Convolution	Number of filters: 128, Filter size: 4, Strides: 1	39	Relu	-
19	Elu	Alpha: 1.0	40	Dropout	Rate: 0.05
20	Batch Normalization	-	41	Dense	Size: 6
21	1D-Max Polling	Filter size: 4, Strides: 2	42	Softmax	-

(B)	
Hyperparameter	Value
Optimizer	Adamax
Learning rate	0.0003
Batch size	128
Epoch number	1000
Validation metric	Accuracy
DL framework	Tensorflow & Keras

Table 10: (A) The overall accuracy of the flow content classifiers for different number of packets in the byte sequence of each flow. (B) The overall accuracy of the flow time series classifiers for different number of packets in the time series of each flow.

(A)		
Num of Pkts in flow byte sequence of each flow	Overall Accuracy(%)	
	FCC-HP	FCC-P
7	79.25	78.50
10	81.52	80.6
12	80.38	79.61
15	81.50	79.72
17	79.95	78.08
20	80.31	78.26

Num of Pkts in time series of each flow	Overall Accuracy(%)	
	FTSC-PS	FTSC-IAT
10	71.94	72.5
25	74.73	74.09
50	74.26	75.02
75	75.38	76.16
100	76.21	76.51
250	75.56	76.79
500	75.66	75.77
750	76.12	75.11
1000	74.73	74.95

B Precision and F-score of packet classifiers under various attacks

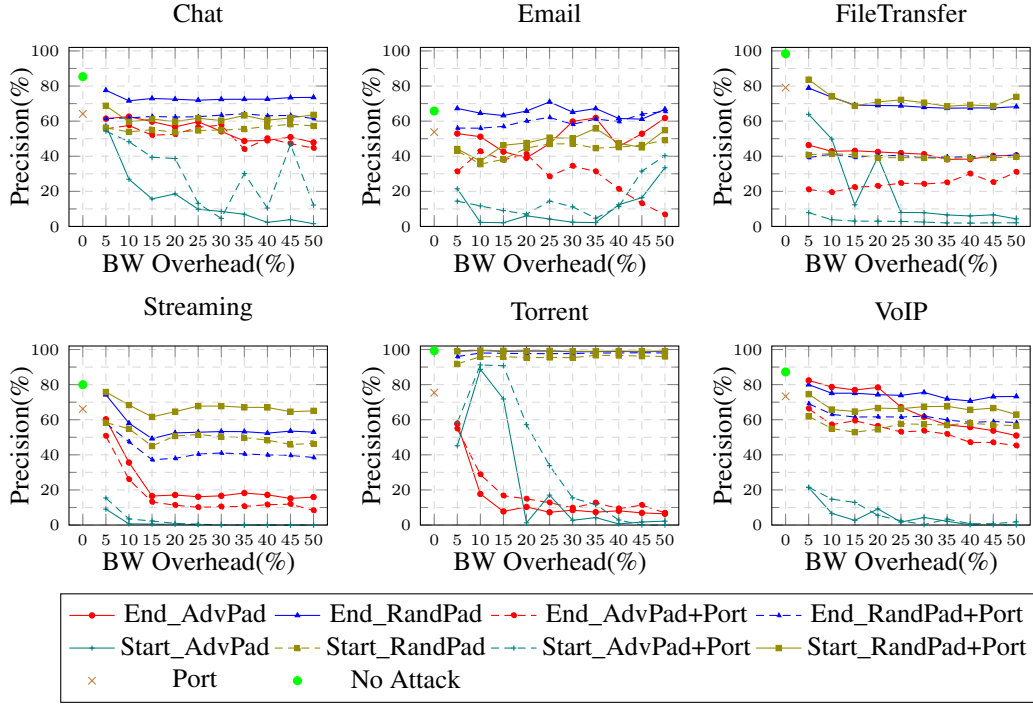


Figure 7: The precision of PC-HP under different attacks over various sizes of BandWidth (BW) overhead. The legends show the kind of attacks that have been applied to PC-HP.

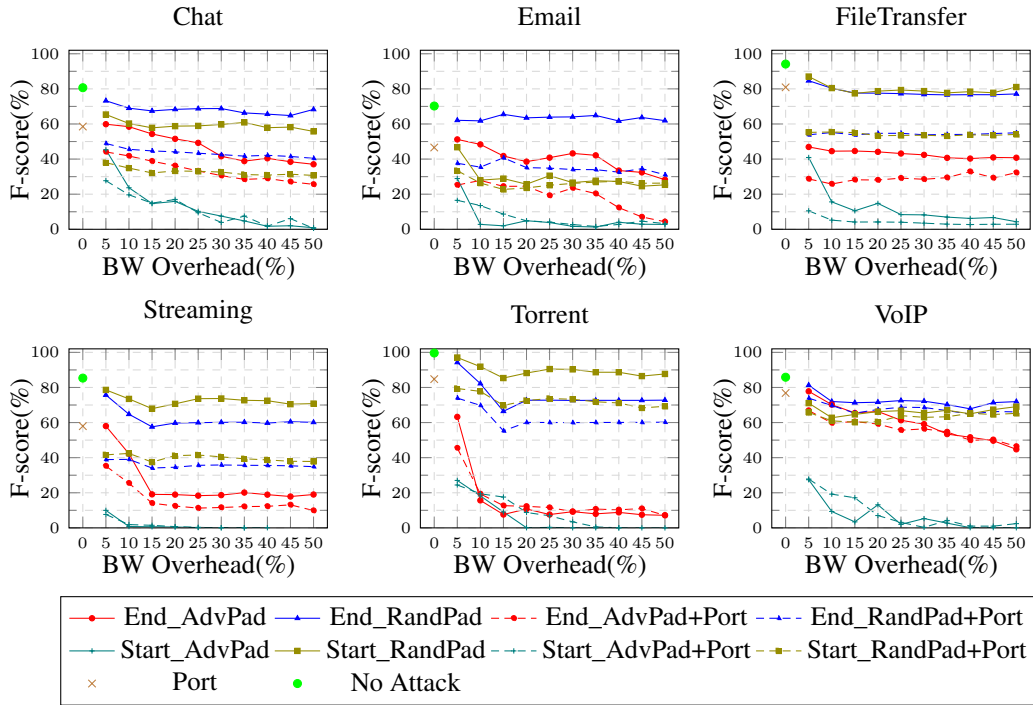


Figure 8: The F-score of PC-HP under different attacks over various sizes of BandWidth (BW) overhead. The legends show the kind of attacks that have been applied to PC-HP.

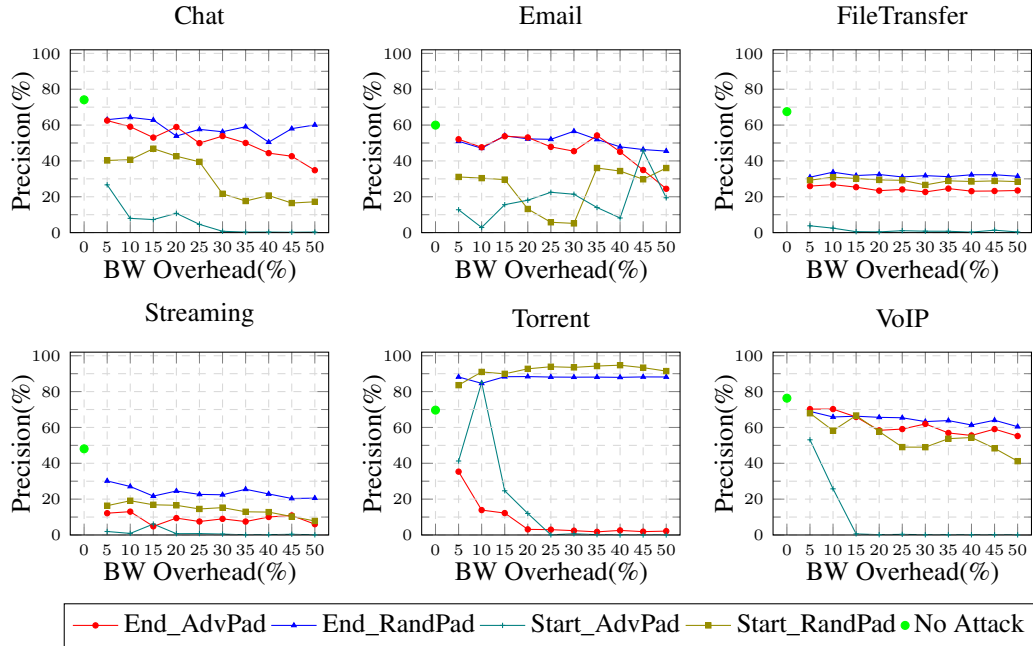


Figure 9: The precision of PC-P under different attacks over various sizes of BandWidth (BW) overhead. The legends show the kind of attacks that have been applied to PC-P.

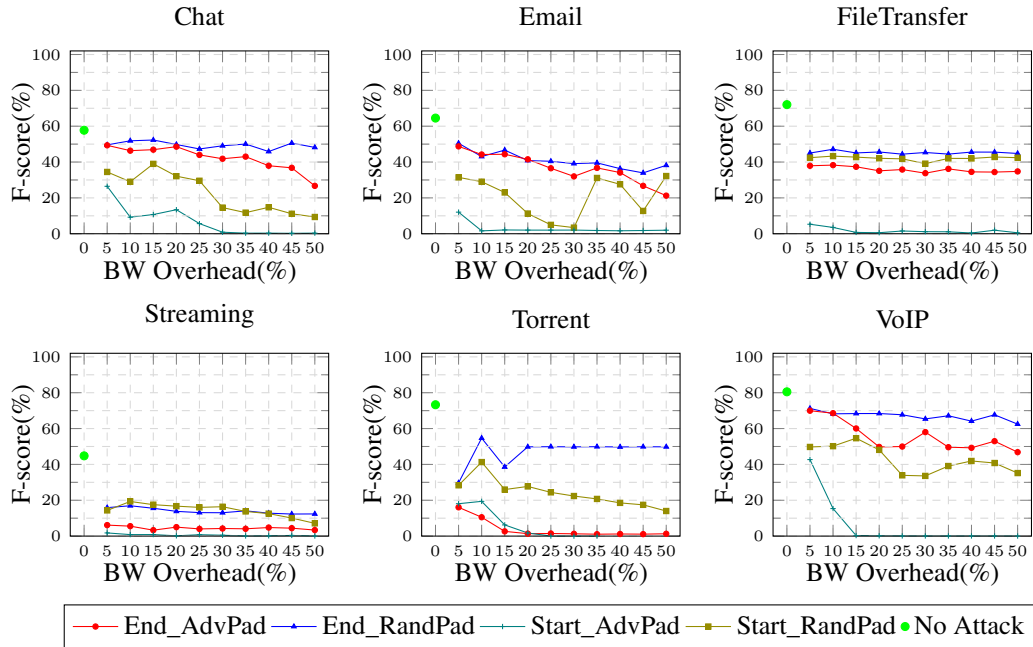


Figure 10: The F-score of PC-P under different attacks over various sizes of BandWidth (BW) overhead. The legends show the kind of attacks that have been applied to PC-P.

C Precision and F-score of flow content classifiers under various attacks

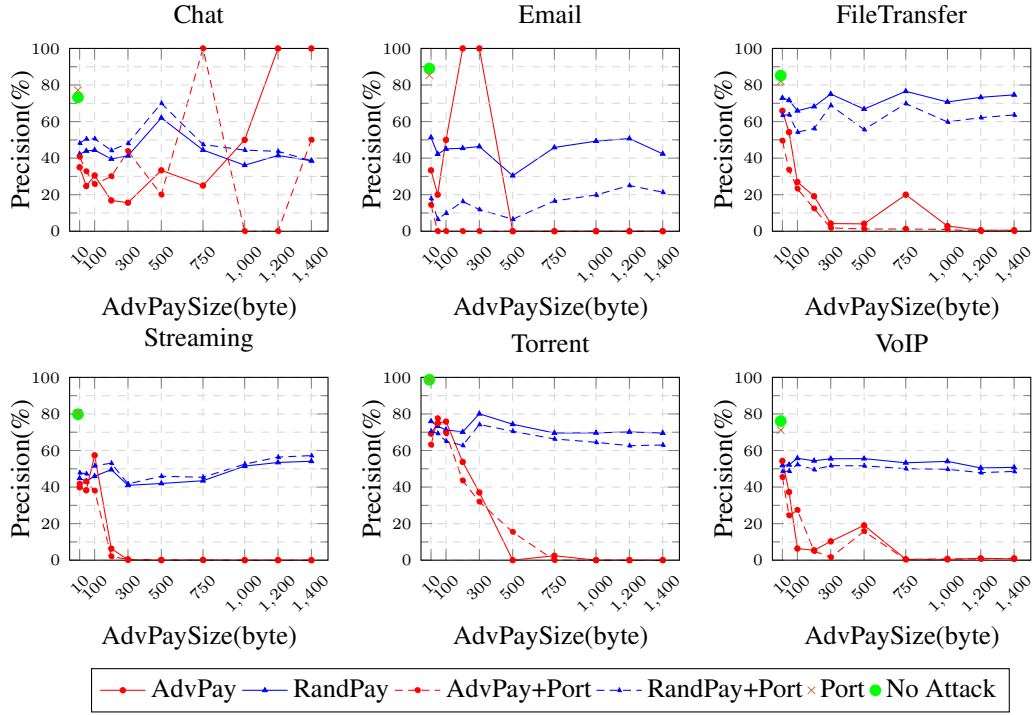


Figure 11: The precision of FCC-HP under different attacks over various sizes of the adversarial payload. The legends show the kind of attacks that have been applied to FCC-HP.

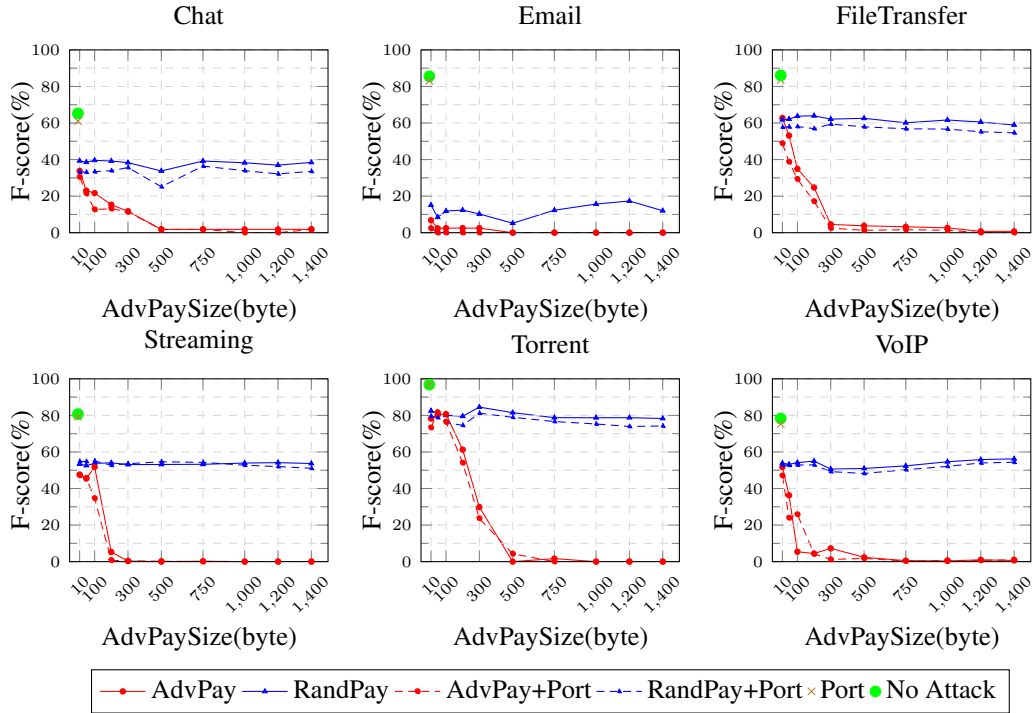


Figure 12: The F-score of FCC-HP under different attacks over various sizes of the adversarial payload. The legends show the kind of attacks that have been applied to FCC-HP.

Adversarial Network Traffic:
Toward Evaluating the Robustness of Deep Learning Based Network Traffic Classification

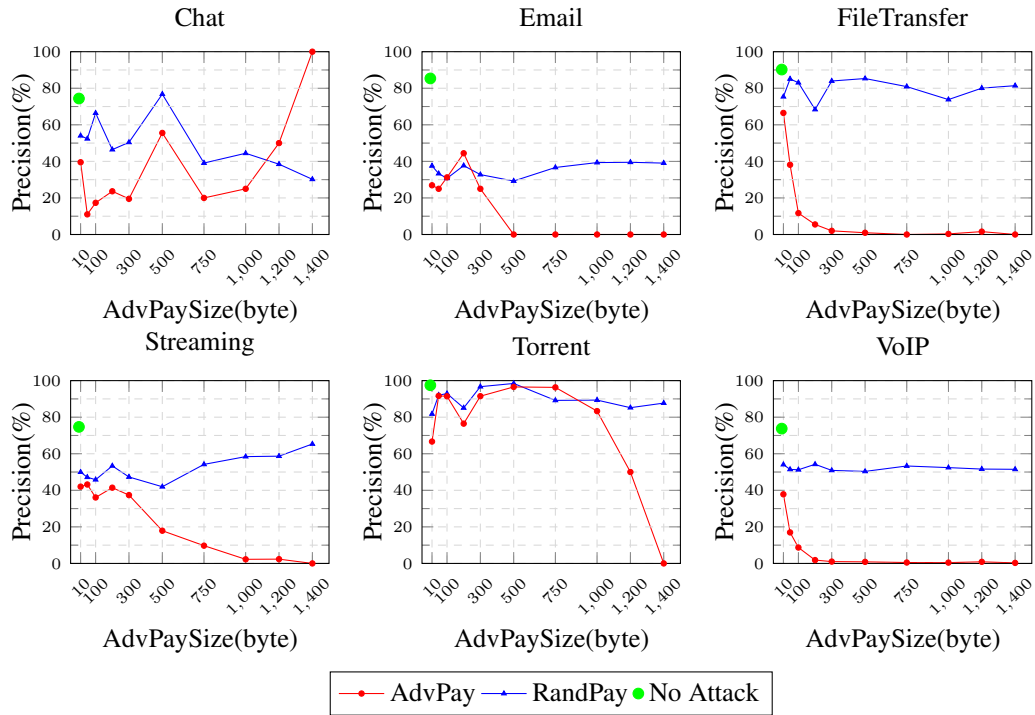


Figure 13: The precision of FCC-P under different attacks over various sizes of the adversarial payload. The legends show the kind of attacks that have been applied to FCC-P.

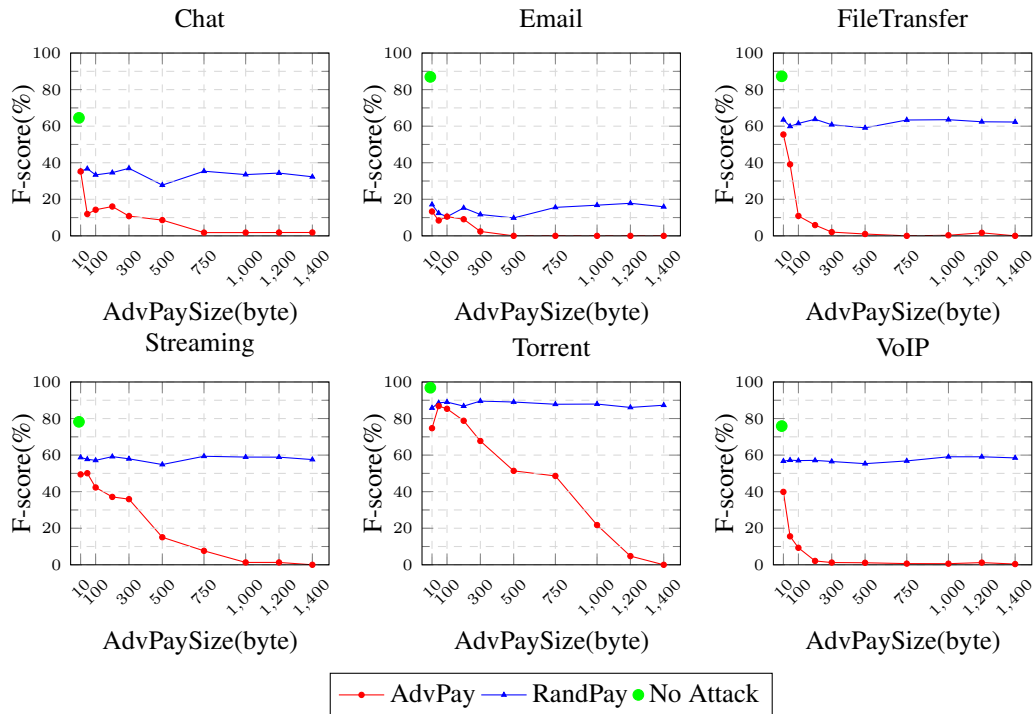


Figure 14: The F-score of FCC-P under different attacks over various sizes of the adversarial payload. The legends show the kind of attacks that have been applied to FCC-P.

D Precision and F-score of flow time series classifiers under various attacks

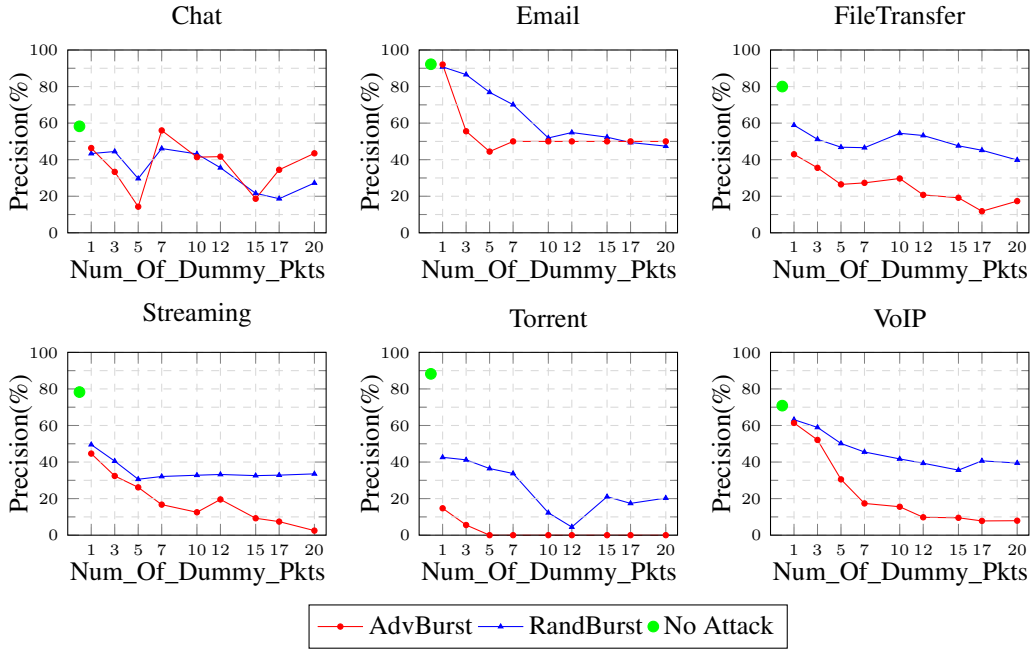


Figure 15: The precision of FTSC-PS under different attacks over the various number of dummy packets. The legends show the kind of attacks that have been applied to FTSC-PS.

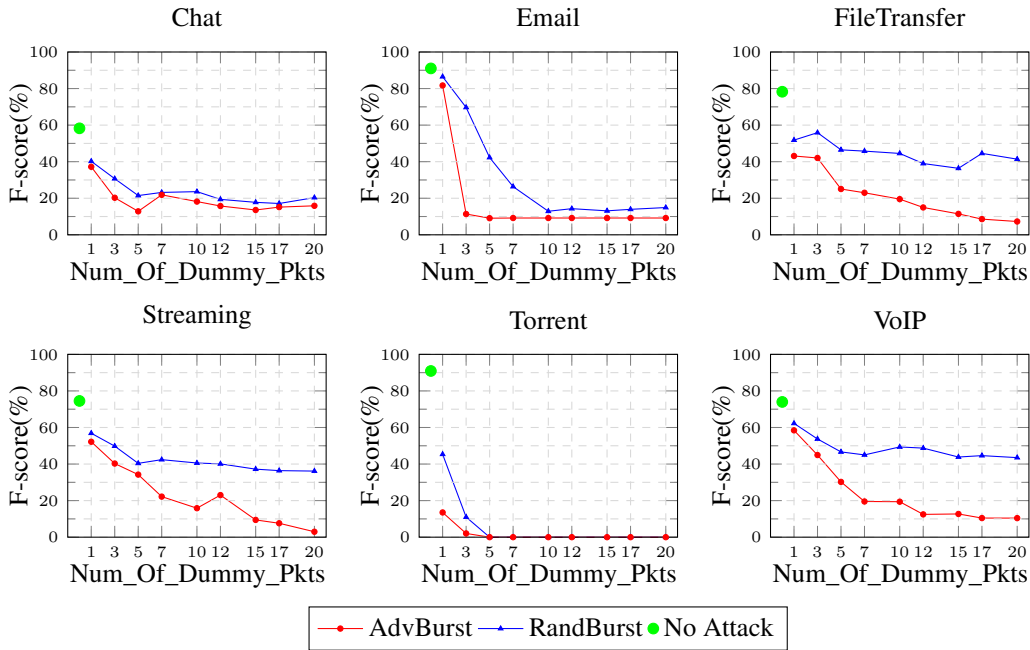


Figure 16: The F-score of FTSC-PS under different attacks over the various number of dummy packets. The legends show the kind of attacks that have been applied to FTSC-PS.

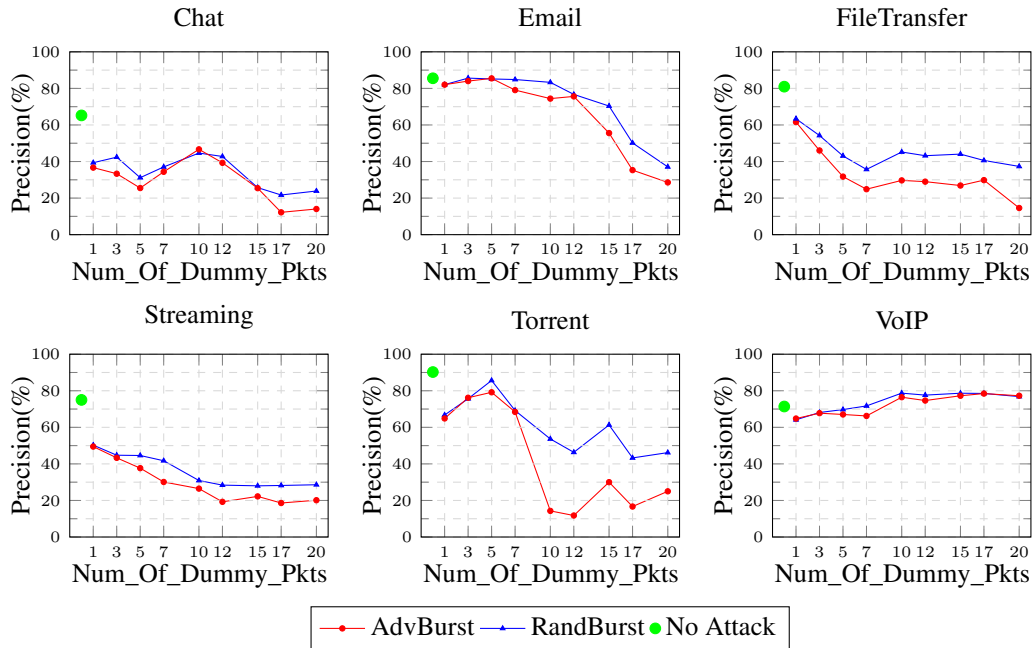


Figure 17: The precision of FTSC-IAT under different attacks over the various number of dummy packets. The legends show the kind of attacks that have been applied to FTSC-IAT.

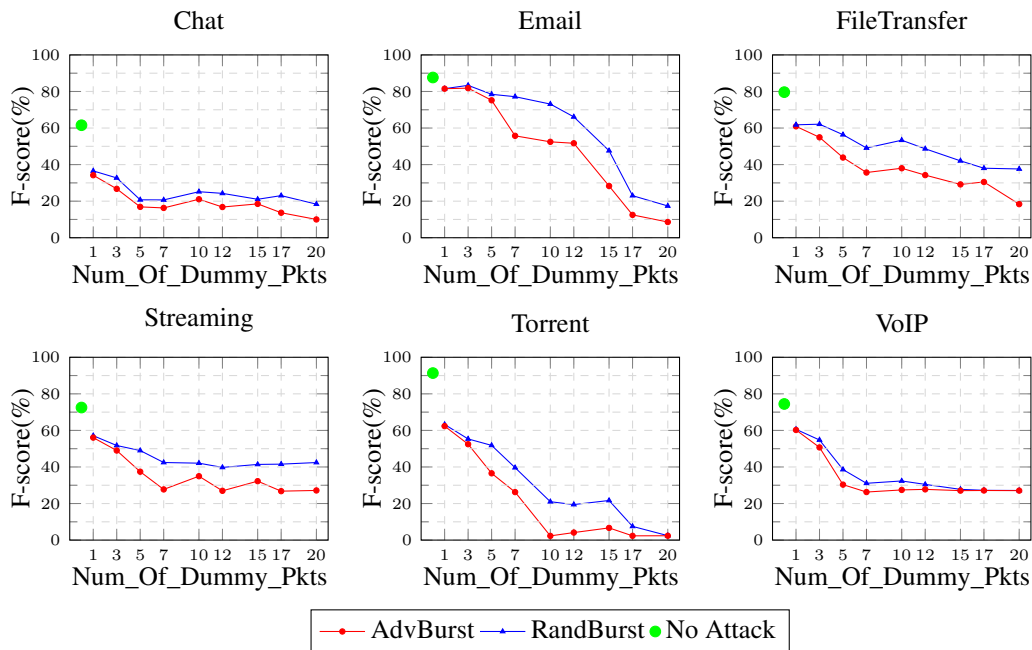


Figure 18: The F-score of FTSC-IAT under different attacks over the various number of dummy packets. The legends show the kind of attacks that have been applied to FTSC-IAT.